

#### Master Thesis

# Application of Directional Antennas in RF-Based Indoor Localization Systems

Dominik Kaspar

September 20<sup>th</sup>, 2004 – March 19<sup>th</sup>, 2005

Supervisor: Prof. Dr. Roger Wattenhofer Support: Dr. Kamran Sayrafian-Pour This report was written in the context of a master thesis at the Swiss Federal Institute of Technology (ETH).

Hereby I affirm that I have written this documentation by myself by any means. All sources used for the thesis on hand are listed completely in the bibliography.

Dominik Kaspar

Gaithersburg MD, United States — March 2005

#### Supervisor:

Prof. Dr. Roger Wattenhofer

#### Support:

Dr. Kamran Sayrafian-Pour (ksayrafian@nist.gov)

#### Student:

Dominik Kaspar (dokaspar@student.ethz.ch)

© 2005 ETH Zürich

## **Abstract**

A simple technique to estimate the position of a given mobile source inside a building is based on the received signal strength. For this methodology to have a reasonable accuracy, radio visibility of the mobile node by at least three access points is required. To reduce the number of required access points and therefore, to simplify the underlying coverage design problem, a new scheme is presented that takes into account the distribution of RF energy around the receiver. In other words, it is assumed that the receiver is equipped with a circular antenna with beamforming capability. In this way, the spatial spectrum of the received power can be measured by rotating the antenna beam around the 360-degree field of view. This spatial spectrum can be used by the receiver as a means for estimating the position of a mobile transmitter. In this thesis, the feasibility of this methodology is investigated, and the improvement achieved in the positioning accuracy is shown.

# **Acknowledgements**

Foremost, I would like to express my thanks to Kamran Sayrafian for his continuing support, interesting ideas and suggestions, his patient explanations and diverting lunch-time conversations.

Many thanks go to Nader Moayeri for giving me the opportunity of writing my master thesis at the National Institute of Standards and Technology in Gaithersburg, Maryland. Also, big thanks to Roger Wattenhofer for giving me the freedom of writing my master thesis abroad.

A great many thanks go out to Matthias 'Mudhold' Wille for his proficient advice and competent help on the MEX typesetting program. Also, special thanks to my brother Peter for his adept math skills.

Last but not least, I would like to express my gratitude to Kate Remely, Mike Mckinley and Marc Rutschlin from the Electromagnetics Division of the National Institute of Standards and Technology located in Boulder, Colorado, for providing the measurement results of the rotating directional antenna.

# **Contents**

Lis	t of F	igures		9
Lis	of Figures         9           t of Tables         11           Localization         13           1.1 Introduction         13           1.2 Definition of Terms         14           1.3 Properties of Localization Systems         16           1.4 GPS         17           1.5 Indoor Localization         18           1.5.1 Multipath Interference         18           1.5.2 Localization Based on Received Signal Strength         20           1.5.3 An Experimental IEEE 802.11-Based Localization System         21           System Model         23           2.1 Spatial Power Spectrum         23           2.2 Raytracing         26           2.3 Beamforming         29           2.4 Experimental Verification Of SPS         31           Simulation Platform         35           3.1 General Overview         35			
1	1.1 1.2 1.3 1.4	Introd Definit Prope GPS Indoo 1.5.1 1.5.2	duction	 13 14 16 17 18 18 20
2	<ul><li>2.1</li><li>2.2</li><li>2.3</li></ul>	Spatic Raytro Beam	al Power Spectrum	 23 26 29
3		Gene Input Buildir 3.3.1 3.3.2 3.3.3 3.3.4 3.3.5 SPS M		35 35 36 37 37 38 38 39 39 40 40 41

#### Contents

		3.5.6 3.5.7	Angle Of Arrival	42 43
4	4.1 4.2 4.3	Comp Anten Anten	rformance Darison Of Distances Measures	49 50
5	Con	clusion	ns	53
A	A.1 A.2	Beam <sup>1</sup> Earth I	tation Details  Iformer: Pattern Generator for Circular Array Antenna  Mover's Distance	56
В	B.1 B.2 B.3 B.4	WiSE Ir WiSE A	ts  neter File Format  nput File Format  mpulse File Format  Antenna Definition File Format  Wall File Format	60 60 61
Bik	oliogi	aphy		63

# **List of Figures**

1.1 1.2 1.3 1.4 1.5 1.6 1.7	Angulation	14 15 15 18 19
2.11 2.12	Simple SPS Example A Sample Radio Map Energetical SPS Shift Angular SPS Shift WiSE Raytracing Illustration of Fast Fading Beamforming With Circular Antennae Gain Patterns of Array Antennas Experiment Setup at NIST (Boulder, CO) WiSE Layout of the Basement at NIST (Boulder, CO) Antenna Patterns Used in Experiment Comparing Simulation Data to Real Measurements. SPS of Two Physically Close Positions	24 25 26 28 29 30 31 32 32 33
3.1 3.2 3.3 3.4 3.5 3.6	Block Diagram of the Simulation Platform Radio Map Creation Process SPS Matching And Performance Evaluation Visualization of the Hausdorff Distance Combining Two Measures Ranked Radio Map Entries	36 39 41 43
4.1 4.2 4.3 4.4 4.5 4.6	Radio Map Resolution	48 48 49 50 51

#### List of Figures

4.8	SPD Plot For Vector Sum Calculation							 52
5.1	Netgear Wireless MIMO Internals						 	 54

# **List of Tables**

	Constant Simulation Parameters	
	Average Position Errors For Evaluated Algorithms	
4.3	Multi-Pass Position Errors	4/
A.1	Core Functions	57
	Visualization Functions	
A.3	Auxiliary Functions	58
B.1	WiSE Antenna File Header	61
B.2	WiSE Antenna File Body	62

## 1 Localization

We're not lost. We're locationally challenged.

John M. Ford

#### 1.1 Introduction

Localization is the momentary process of determining the position of an object, whereas tracking refers to a continuous observation of an object's movement. With evolving wireless technologies, localization and tracking of mobile devices has become an increasingly attractive area of research and development. Current systems in use, such as GPS (details in Section 1.4), provide reliable and highly accurate localization in outdoor environments and permit location-aware services in our every-day lives. Examples include naval navigation, air traffic control, and personal destination-finding systems in automobiles. Another significant application of such technologies is in emergency situations where it is important to be able to track the movements of first responders or to locate a victim. Downtown and indoor environments pose much harsher conditions for accurate localization, because of interference and objects blocking the communication channels. This thesis is an attempt to improve indoor localization by persuing a novel approach using directional antennas.

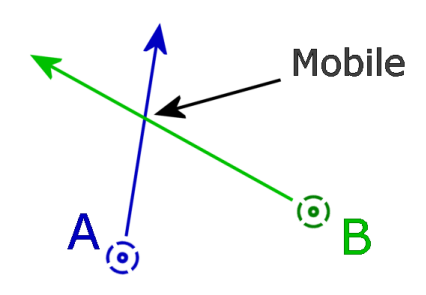
Although localization systems always serve the same fundamental purpose — to find the position of an object or person — they can vary in many ways. A multitude of factors come into play when trying to classify location system implementations. This chapter first defines a few important terms used throughout this document, then outlines a reasonable approach to characterize or evaluate localization systems and ends with a summary of the implementations and techniques most prevalent in the literature.

In Chapter 2 a new scheme for indoor localization is presented, including the methods and models used for a theoretical analysis. Chapter 3 then explains the simulation platform, which has been established for performance evaluation. In Chapter 4, the simulation results are presented and Chapter 5 finally closes with some concluding remarks.

#### 1.2 Definition of Terms

#### **Lateration and Angulation**

In order to calculate a position from a known set of distances or angles, methods such as *lateration* and *angulation* are often used in localization techniques. As Figures 1.1 and 1.2 depict, it is possible to estimate a position in 2D from either two given angles or three known distances. For the 3D case, additional values are needed.



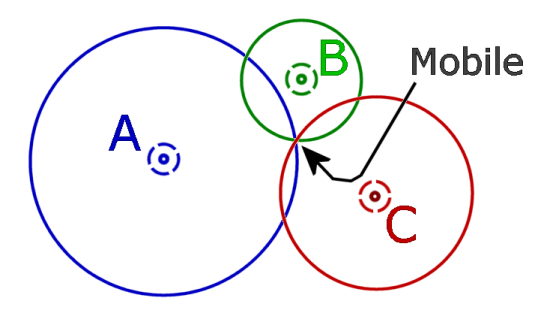


Figure 1.1: Angulation.

Figure 1.2: Lateration.

#### **Azimuth and Elevation**

Azimuth and elevation together can in principle specify any direction (see Figure 1.3). *Azimuth* is defined as the horizontal angle measured clockwise from north and ranges from 0° to 360°. Elevation is the angle by which an object is lifted above the horizontal plane and ranges from -90° (straight down or *nadir*) to +90° (straight up or *zenith*).

#### **Antennas**

An antenna is a structure for radiating or receiving electromagnetic (EM) waves that carry information. For wireless communications, EM signals are not sent through a transmission line. Antennas are therefore required for the transmission and reception of the signals. An antenna gain pattern is the variation of field intensity as an angular function around an antenna. Gain patterns are usually represented graphically for the far-field conditions in either the horizontal or vertical plane as a plot of signal strength vs. azimuth or elevation (see Figure 1.4). The antenna gain is a measure of how much the input power is concentrated in a particular direction. It is expressed with respect to a hypothetical ideal antenna, which radiates equally in all directions. There are two basic categories of antennas:

**Omnidirectional** antennas radiate the same amount of energy in all horizontal directions. Their horizontal gain pattern is therefore a circle. The vertical gain pattern may be of any shape.

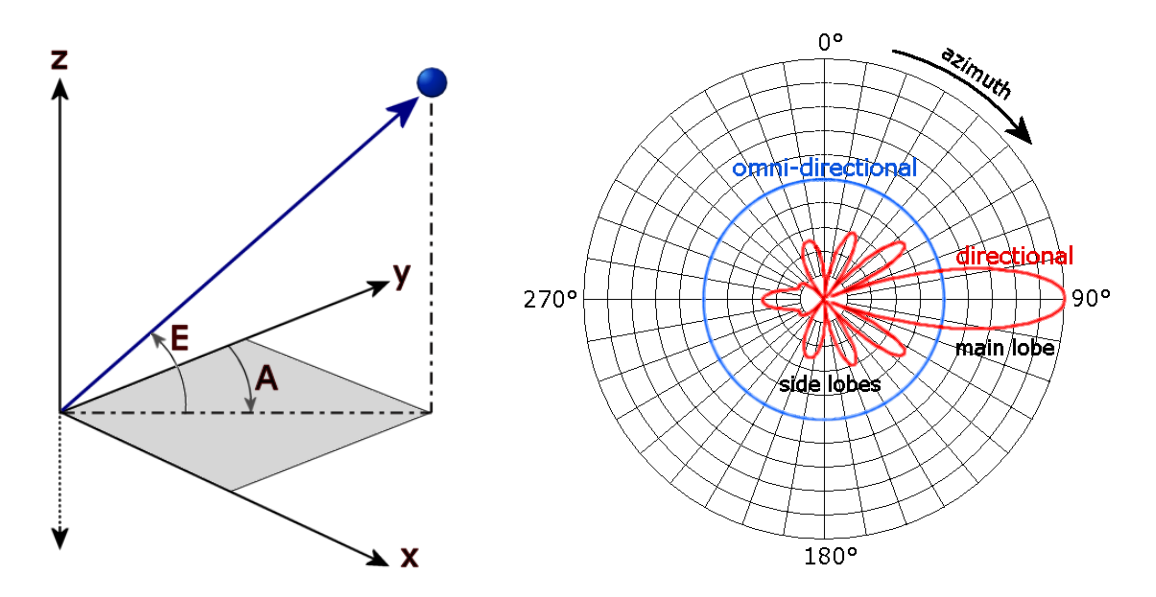


Figure 1.3: Azimuth and elevation.

Figure 1.4: Antenna gain patterns.

**Directional** antennas are designed to have a gain in one particular direction and a loss in others. They have a narrow central beam of high gain, the so called *main lobe*. The other smaller local maximums are called *side lobes*, and directions in which the signal strength is zero are called *nulls*.

#### Free Space Path Loss

Propagation of waves in free space is different from that in cables. With respect to signal propagation, a wave does not lose from its total energy as it travels, except as a result of absorption or scattering. In three dimensions waves radiate spherically. As they travel, the surface area they occupy increases as the square of the distance traveled. However, since energy is conserved, the energy per unit surface area must decrease as the square of the distance. Thus the power of free space waves obey an inverse square law. For each doubling of the distance between the source and receiver, a 6 dB loss is experienced. For all frequencies up to millimeter-wavelength frequencies, this free space loss is the most important source of loss. Because of it, wireless systems usually require much more power than cable or fiber systems.

#### **Signal Propagation**

The following list describes different effects a signal can be influenced by when traveling from a transmitter to a receiver:

**Reflection** occurs when a wave meets a plane object. The wave bounces back without distortion; the angle of incidence is equal to the angle of reflection.

- **Refraction** happens when a wave penetrates a medium of different wave speed. The direction and speed of the wave are altered.
- **Diffraction** occurs when the wave encounters an edge. The wave has the ability to turn around the corner of the edge. Diffraction is dependent on frequency the higher the frequency, the less diffraction. Very high frequencies (e.g. light) hardly diffract at all.
- **Scattering** is a catch-it-all category of wave interactions that are too complex to be described as reflection, refraction or diffraction. Typically the result of scattering is to heavily attenuate the wave and reradiate it over a wide range of directions. Scattering too is strongly frequency dependent and usually increases with higher frequencies.

#### 1.3 Properties of Localization Systems

The following is a collection of attributes which can be used to characterize any localization system. The listed attributes are generally independent of a particular system's techniques and technologies. And even though they are not equally applicable to every system, the classification features form a meaningful set of properties for a localization system (12).

- **Physical vs. Topological** There are two different ways of displaying information about the current position of an entity. Position estimates in latitude, longitude and altitude or cartesian coordinates (i.e. (x,y,z), such as Universal Transverse Mercator (UTM)) are *physical* locations, while designations like "in the conference room" or "in aisle 12 of storage room C" are of *topological* nature.
- **Absolute vs. Relative** A localization implementation with *absolute* position information has a common reference system (such as latitude/longitude), while *relative* positioning occurs according to a local origin. For example, a transportation truck could use the Global Positioning System (GPS) to find the way to its destination, while a safety system is used to measure the distances relative to other vehicles on the highway.
- Central vs. Local Computation Some localization systems carry out the relevant computations on a *central* machine, other implementations require every mobile node to have a *local* processor. While centrally managed location systems can omit expensive mobile equipment, there remains an issue of privacy. A mobile node might not want any other instance to have access to its current whereabouts.
- **Accuracy and Precision** All localization systems can be evaluated to obtain a notion of how well an object can be located. For example, inexpensive GPS receivers can estimate their location to a resolution of 10 meters, but more

- expensive ones have an *accuracy* of 1 to 3 meters. On the other hand, a system with high *precision* achieves its accuracy with a high probability.
- **Scale and Scalability** Large-scale localization like GPS covers the entire planet, while systems of smaller *scale* might only work in a downtown area or in a warehouse. The infrastructure size of a localization system defines its scale, while its *scalability* is limited by how difficult it is to extend the infrastructure.
- **Recognition** Some localization systems are not only required to find a position, but also need to *recognize* the kind of object in question. For example, readers in a warehouse might be challenged to find an object of a certain type or quantity.
- **Cost** Many factors affect the *cost* of a localization system, such as the time of installation, administration needs, price per mobile unit and the complexity of the infrastructure.
- **Limitations** Some systems do not work in certain environments or under special circumstances. GPS for instance is unable to locate any receiver inside of buildings, because the satellite signals are too weak to penetrate walls.

#### 1.4 **GPS**

GPS is a satellite-based navigation system that uses a network of 24 devoted satellites placed into orbit between 1978 and 1994 by the United States Department of Defense. Originally intended as a military system, the US government made it available for civilian use in the 1980s. As they travel, the GPS satellites are constantly transmitting low-power radio signals (= 50 watts) to the earth's surface. These signals are picked up by GPS receivers which process the information from two satellites and calculate the exact two-dimensional position of the user through triangulation. If three or more signals are captured by the receiver, a precise three dimensional location can be calculated.

Differential GPS (DGPS) is a land-based system, in which ground towers receive GPS signals and transmit them with error correction. The DGPS system works by placing a series of GPS receivers at precisely known locations. Since the reference station knows its exact location, it can determine the errors in the satellite signals by comparing the received signal with the expected (correct) signal. These signal differences can then be applied to the signals the DGPS receiver gets from the satellites. With this form of error correction, DGPS accuracy is 1 to 5 meter.

Traveling by line of sight, the GPS radio signals are incapable of penetrating most solid objects, and as such GPS cannot be used underground, or inside buildings. The next section discusses different techniques used for localizing objects in places GPS cannot provide coverage.



Figure 1.5: A GPS satellite in orbit

#### 1.5 Indoor Localization

As previously mentioned, the problem of localization is a lot more difficult inside of buildings. The reason for this is that signals get affected by objects (such as walls, furniture and even people), as opposed to outdoor environments where signals usually travel on direct *line-of-sight* paths.

#### 1.5.1 Multipath Interference

Interference caused by signals bouncing off the walls and other obstacles and arriving at the receiver at different times is called *multipath interference*. The relative phase of multiple reflected signals can cause constructive or destructive interference at the receiver. This is experienced over very short distances (typically at half-wavelength distances), thus it is given the term *fast fading*. These variations can vary up to 20 dB over a short distance. Indoor environments are so called *multipath channels*, because the communication channels which connect transmitters with receivers are affected by multipath interference (see Figure 1.6).

The following list is an overview of different approaches to tackle the problem of indoor localization. For each category, an existing localization system is briefly described.

**Infrared** The first indoor badge sensing system, the Active Badge (25) location system, which was developed at Olivetti Research Laboratory, now AT&T Cambridge, consists of a cellular proximity system that uses infrared (IR) technology. IR emitters and detectors can be made very small and cheaply and

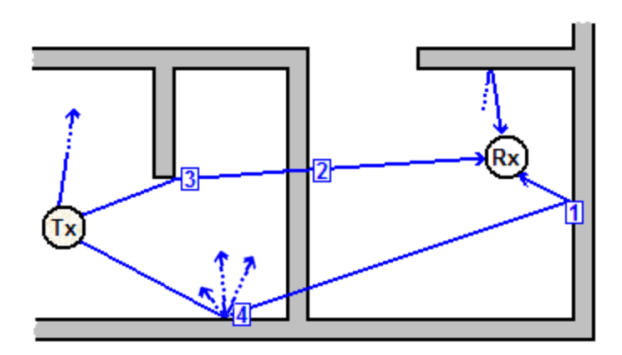


Figure 1.6: *Multipath Channel* - Phenomena such as reflection (1), refraction (2), diffraction (3) and scattering (4) cause interference of RF signals.

are capable of operating within a 6 meter range. In the Active Badge system, each badge emits unique codes every 15 seconds, which are picked up by a network of sensors placed around the indoor environment. A central station polls the sensors for badge sightings, processes the data, and then makes it available to clients that may display it in a useful visual form.

**Ultrasound** Much higher accuracy can be achieved by a location system called Active Bat (26; 9), which uses ultrasonic pulses to estimate distance. Receivers that are fixed to the ceiling in a precise grid estimate the position of the transmitting *Bats* by time-of-flight multilateration. The Active Bat system impresses with a high accuracy of 9 cm in 95% of the time, but the disadvantages are its high costs and low scalability. In another system called Cricket (19), *listeners* transmit both ultrasound and radio frequency signals concurrently. The distance to any beacon in range can then be calculated using the time difference of arrival between the RF signal (which travels at the speed of light) and the ultrasound signal. Cricket reliably locates beacons within topological regions of 4 by 4 feet.

**Electromagnetics** Electromagnetic trackers like Flock of Birds (1) can determine object locations and orientations to a very high accuracy and resolution (around 1 mm in position and 0.2° in orientation), but they are expensive and have a short range (within a few meters). Electromagnetic methods also suffer interference from monitors and metal structures. Initially developed for use in mobile military vehicles as a head-tracking device, their field of application now also includes biomechanical measurement of anatomical parts or even hand tracking in video games.

**RF Signal Strength** A simple approach to tackle the problem of indoor localization is by building a database of received signal strength (RSS) values throughout a given environment. Even with inexpensive off-the-shelf equipment using IEEE 802.11 wireless LAN technologies, localization systems can be built that achieve 3 meter localization accuracy (5). A prime example of such

a system is RADAR (2), which closely follows the methodology described in Section 1.5.2.

Another interesting RSS-based localization methodology has been proposed in (15; 16) where a probability distribution is constructed during the training phase. Considering the fact that received signal strength can vary over time at a constant location, recording an entire signal strength distribution might lead to better localization performance as opposed to only storing its mean value. Then, a Bayesian inference approach is used to estimate the mobile's coordinates with the highest probability.

A true RF localization technique is presented in (14): a simple algorithm for computing the location of a device based on signal strengths from FM radio stations. The system is capable of locating devices down to suburb-sized areas with a precision of 80%.

A commercially available and conveniently testable indoor positioning tool can be found in (4); it claims to feature up to 1 meter average location accuracy, but its implementation details are not public.

Computer Vision In the publications (22; 23) an interesting robot called MOPS (MObile Post System) is presented, which is able to autonomously deliver mail in office buildings. MOPS uses range sensors to extract landmarks (such as walls) and is able to solve the problem of self-location by reading door number plates using a camera. Only 750 milliseconds are used for the recognition phase (which is implemented with a neuronal network), thus enabling the robot to work in real-time.

RFID Radio frequency identification (RFID) is a method of remotely storing and retrieving data using devices called RFID tags. An RFID tag is a small object, such as an adhesive sticker, that can be attached to or incorporated into a product. RFID tags contain antennas which enable them to receive and respond to radio-frequency queries from an RFID interrogator. RFID tags are often envisioned as a replacement for bar codes, but potential usage of this technology is quite unlimited. For instance, in (8) it is shown that RFID tags can also be used to accurately localize mobile robots in an office environment.

Physical Contact A very different approach has been followed in the Smart Floor (17) project, in which an indoor floor area is covered with a grid of force measuring sensors to capture footsteps. Even though Smart Floor is costly and has poor scalability, it not only serves localization but it is also capable of recognizing individuals by their footfalls.

#### 1.5.2 Localization Based on Received Signal Strength

In the context of this thesis, RSS-based localization refers to the technique of estimating the position of a mobile device by comparing a signal strength fingerprint to a pretrained database. The general philosophy in this approach

is to establish a one-to-one correspondence between a given position and the average received signal strength from at least three transmitters. There are two main phases in the operation of an RSS-based system: an *offline* phase (i.e. data collection or training phase) and an *online* phase (i.e. real-time mobile position estimation).

Before real-time localization can take place, signal strength measurements have to be conducted at a number of known locations. The collection of all these measurements, called a *Radio Map*, is an approximation of the radio properties inside the survey area. More precisely, for every point  $A_i$  in the radio map a collection of values  $(x_i, y_i, z_i, RSS_1, ..., RSS_n)$  is recorded, where  $(x_i, y_i, z_i)$  are the physical coordinates of the trained point  $A_i$ , and  $RSS_k$  is the mean signal strength obtained from the kth out of n access points in the survey area. More elaborate radio map designs can also include a standard deviation value of the received signal strengths, or even distinguish different directions a user can face at each training location. For example, every entry  $A_i$  in the radio map could contain tuples of the form  $(x_i, y_i, z_i, d, RSS_1, ..., RSS_n)$ , where  $d \in \{N, E, S, W\}$  is one of four possible orientations of the recording device when conducting the measurements.

After a full radio map of an indoor environment has been generated, it is possible to use that database for localization purposes. Once a mobile node has obtained signal strength values of access points in its vicinity, it can compare that vector to all the entries in the radio map in order to find a closest match. In the searching process, the algorithm computes the Euclidean distance between each signal strength tuple  $(RSS_1,...,RSS_n)$  in the radio map and the measured signal strength tuple  $(RSS_1',...,RSS_n')$ . It then picks the radio map entry that minimizes the distance in signal space and declares the corresponding physical coordinates as its estimate of the mobile's location. Variations, such as calculating the k best matches and averaging their locations, are also common.

#### 1.5.3 An Experimental IEEE 802.11-Based Localization System

In a previous project at the National Institute of Standards and Technology (NIST), I have implemented the localization system (13), described in (7). The program, implemented in Java™, features a graphical user interface on which a building floorplan can be displayed, and a graph of training points (nodes) and possible transitions between them (edges) has to be defined. The user does not need to be aware of the access point locations, since the localization method is based on fingerprints only; the absolute signal intensity values are irrelevant. After this initial step, the system has to be trained as described in Section 1.5.2. A fully trained system can then be toggled into the real-time localization mode, in which a marker on the screen indicates the current position of the mobile. From experience in

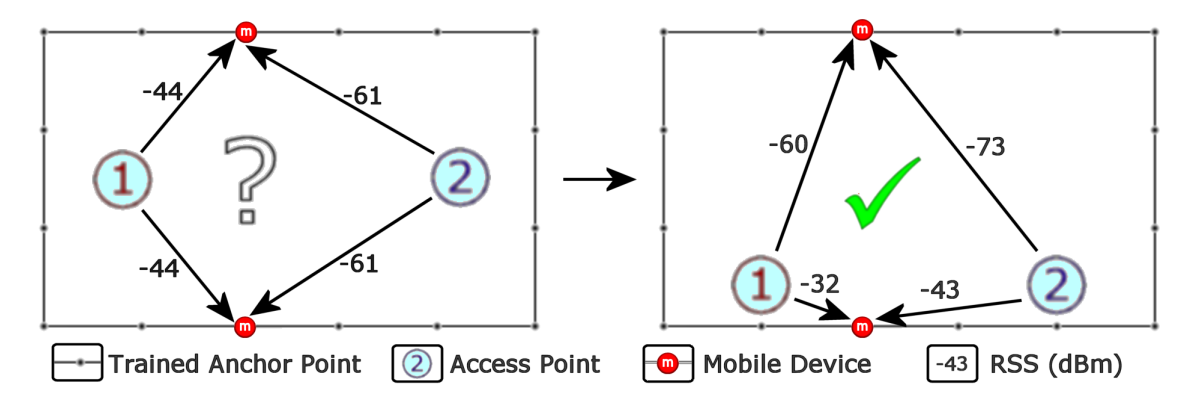


Figure 1.7: If anchor points are placed in a one-dimensional fashion, localization is feasible with less than the usually required number of 3 access points. A strategical placement of the access points is essential.

many tests and demonstrations, the following conclusions can be drawn:

- The system performance varies over time. Even though the system is still able
  to provide localization information a month after it has been trained, its accuracy is suffering from changes in the environment. Especially in environments where access points get turned on and off, or even change MAC
  addresses, a trained system might be useless even shortly after it has been
  trained.
- One-dimensional anchor point placements lead to higher localization precision than two-dimensional grids. For instance, if the trained area consists of a long hallway or several interconnected hallways (as used in many publications), localization accuracy is much higher, because for most locations, two access points suffice to get a reasonable estimate. Figure 1.7 schematically shows a collection of trained points in a (one-dimensional) rectangular hallway with two access points providing signal strength values. Symmetrical placement of the access points leads to localization ambiguity, because at least two points exist which obtain equal RSS readings. In this case, a third access point would be needed for unique estimates. But because all trained points are arranged one-dimensionally, the problem of ambiguity can be solved by asymmetrical access point deployment.

# 2 System Model

#### 2.1 Spatial Power Spectrum

The proposition in this thesis is to follow the same two-phase approach as the general RSS-based localization method mentioned in Section 1.5.2. However, instead of recording received signal strength only, additional information about the distribution of the received power around the corresponding location is incorporated into the signatures which form the radio map. By exploiting this additional angular data, increased localization performance is expected. The hypothesis is, that by combining signal strength with directional information, only one access point would suffice for localization accuracy comparable to methods based on RSS only.

A so called *spatial power spectrum* or *SPS* describes the received signal strength with regard to orientation at a fixed location. An SPS is basically a two-dimensional graph of the received power versus azimuth. Omnidirectional antennas obtain equal signal strength in all directions and are therefore unable to measure power distributions. On the other hand, directional antennas receive varying signal strength when their orientation changes and are thus suited to generate spatial power spectra. By rotating a directional antenna around its 360° field of view, while conducting signal strength measurements at discrete angular steps, spatial power spectra can be obtained for a desired location. Each point on an SPS plot indicates the received power when the main lobe of the antenna is directed toward the corresponding azimuth. The application of circular array antennas with beamforming capability (more on this topic in Section 2.3) is a very promising method for generating spatial power spectra.

Figure 2.1 shows a simple two-dimensional scenario, including an omnidirectional transmitter (Tx) and a receiver (Rx) using a directional antenna. The walls in this example have a high attenuation; that is why there are only two main paths that a signal can travel. Once the receiver generates the SPS by rotating its main lobe in all azimuth directions, it will detect signal intensity peaks at about 220° and 305° azimuth. Even though there are no incoming signals from certain azimuth angles (for instance at 90°), the antenna still receives a signal when it is oriented in such directions. This is due to the antennas side lobes, which are detecting signals from other directions, even though they might be many dB weaker than if obtained by the main lobe.

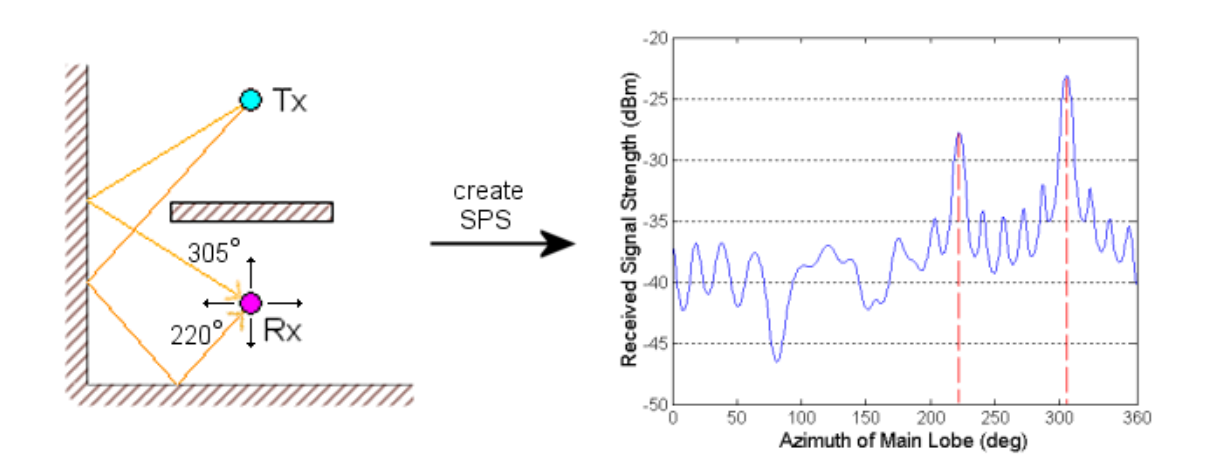


Figure 2.1: A simple illustration of an SPS

Now, the problem is to first form a database of the measured (or calculated) spatial power spectra at the points of interest. Figure 2.2 shows how a radio map has been compiled by generating an SPS at every intersection point on a grid with 2 meter spacing. This is the training phase which essentially yields more sophisticated fingerprints of locations in the building as opposed to measuring just the average received signal strength.

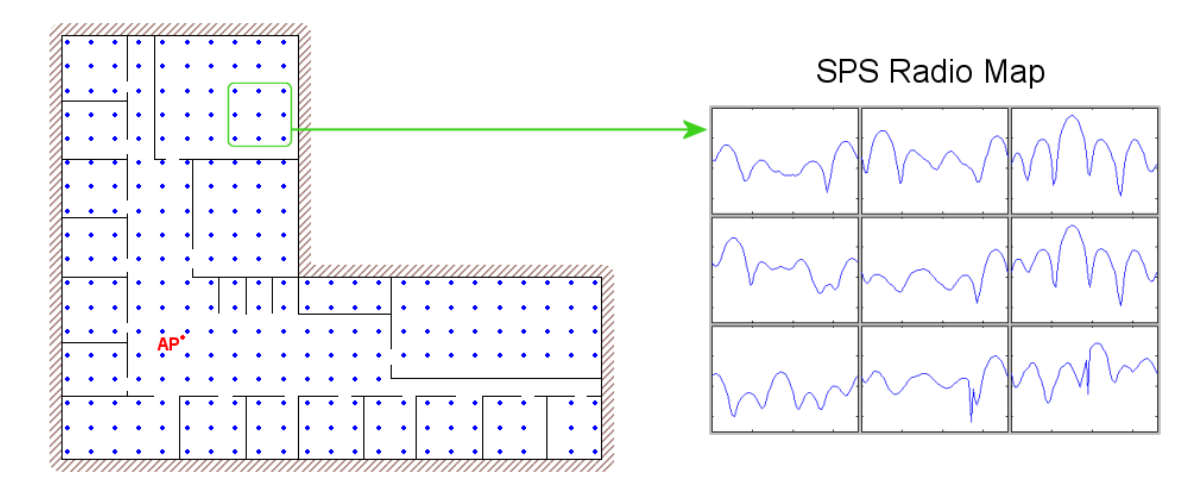


Figure 2.2: A sample radio map

Once the SPS data for a set of pre-determined points is collected, the test and verification phase of the positioning system can begin. Essentially, each SPS graph that is obtained per access point can be regarded as a spatial signature that signifies the position coordinates of the mobile as seen by that access point. If an SPS of an unknown point inside of this layout is measured (or calculated) it

can be compared to all the entries in the radio map and the position of the best match would be a good estimate for the unknown location. On the contrary to the RSS-based methodology, where a  $L_2$  distance is used to establish a metric between two RSS vectors, the problem of finding the closest match to a given SPS is not so obvious.

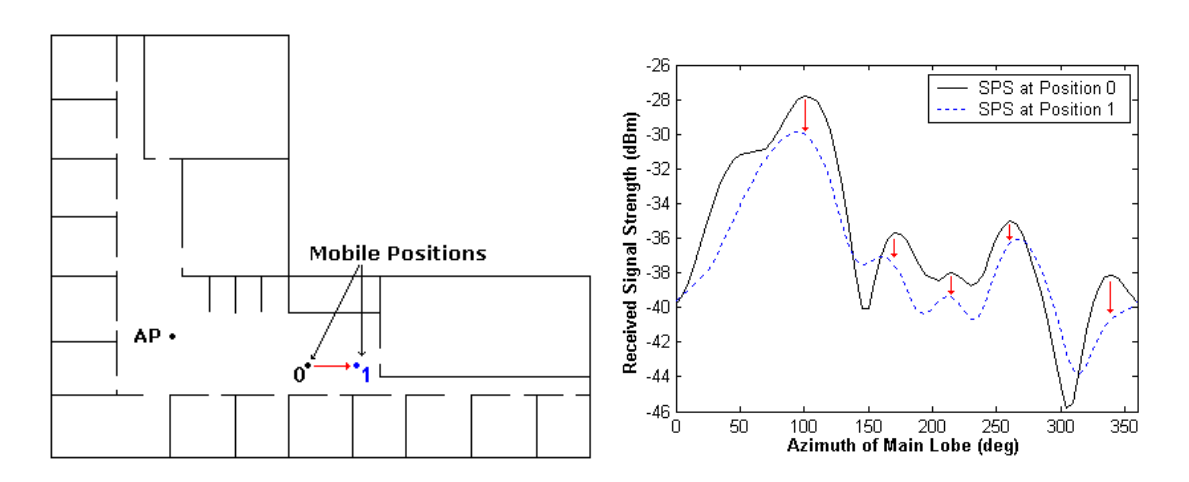


Figure 2.3: Energetical SPS Shift

To further elaborate on this problem, consider the scenarios depicted in Figures 2.3 and 2.4. In these examples, the mobile is the transmitter and the access point is the receiver equipped with a circular array antenna. Figure 2.3 displays the SPS observed by the access point when the mobile position changes from 0 to 1. Since the mobile distance from the access point is increased, the SPS graph decreases in magnitude while generally maintaining its shape.

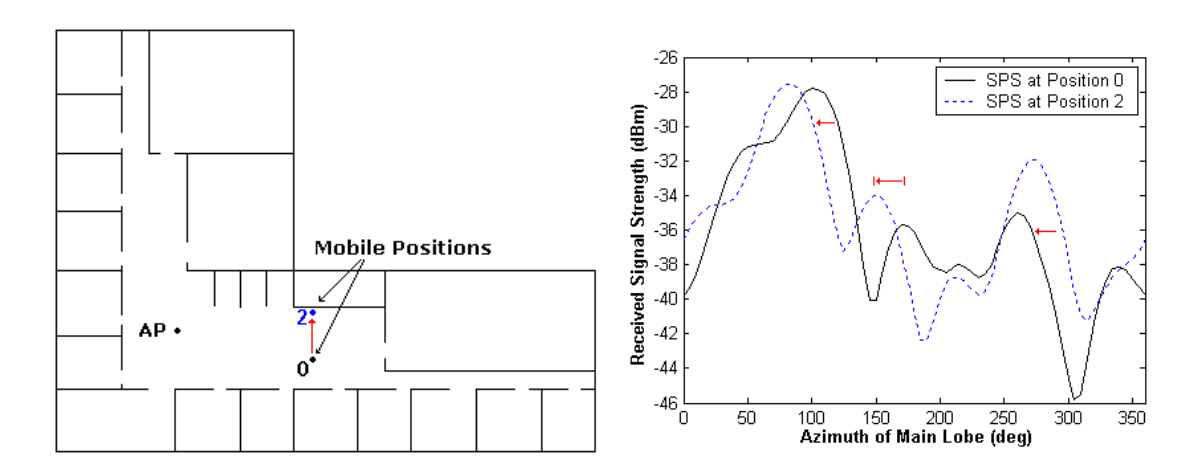


Figure 2.4: Angular SPS Shift

Figure 2.4 shows the scenario where the mobile device changes its position from

0 to 2. In this case, the distance of the mobile node to the access point is almost unchanged; however, the direction from which the access point receives the RF signal is now different. This translates to an angular shift in the spatial signature. In short, physical proximity in mobile positions translates to visual similarity in the spatial signatures seen by an access point. Although it can be shown that this is not true at all times, the methodology outlined here is still applicable under all circumstances. In order to measure the similarity between two signatures, a distance metric has to be chosen that is capable of considering both of the above situations. One such metric is the Earth Mover's Distance (EMD), which will be explained in Section 3.5.5.

#### 2.2 Raytracing

This thesis investigates the feasibility of SPS-based localization by implementing a simulation platform that matches the condition of an indoor environment. The main difficulty in simulating an indoor RF channel is the strong dependence of the received signal on the layout of the building (i.e. multipath channel). In particular, all walls, windows, and other objects that affect the propagation of RF waves will directly impact the signal strength and the directions from which RF signals are received. Empirical, statistical, and deterministic models have been used to describe the behavior of such multipath channels (10). In this study, a sophisticated raytracing tool has been elected to predict the received signal in an indoor RF channel. Wireless System Engineering (WiSE) (6) is a raytracing tool that has been developed and verified by Bell Laboratories.

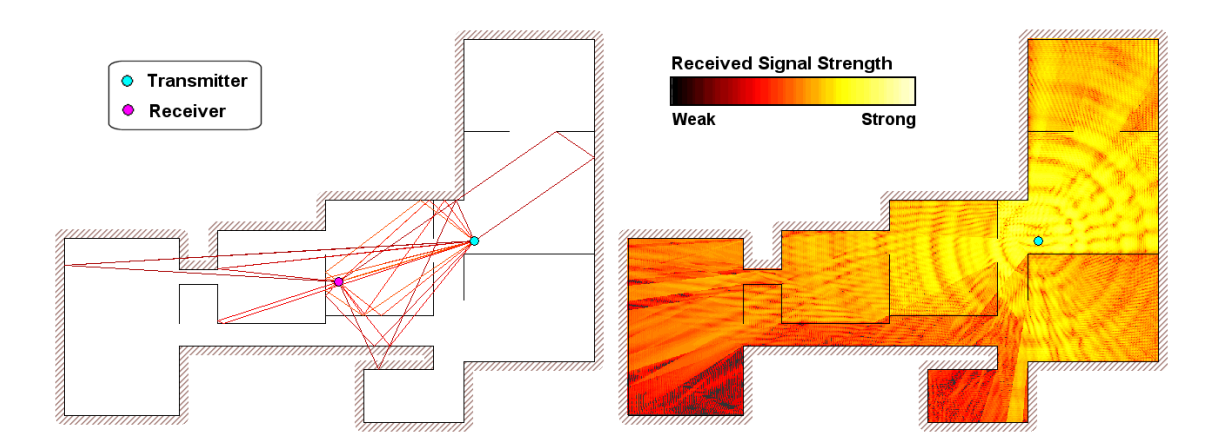


Figure 2.5: Raytracing with WiSE.

Figure 2.5 shows a pictorial sample of the multipath signal for a given floor layout and a given transmitter/receiver location obtained through the raytracing tool. It is understood that even such models have limitations in their accuracy and

are also subject to errors when there are changes in the environment, such as furniture moving, or even people walking through the building; however, this approach will give an opportunity to create a testbed that, to the extent possible, mimics the conditions of a real-life indoor channel.

The raytracing tool is capable of providing the impulse response of a stationary channel in the following form:

$$h(t) = \sum_{k=1}^{N} a_k \delta[t - t_k] e^{j\theta_k}$$
(2.1)

N: number of multipath components (rays)

 $a_k$ : amplitude of the received impulse on path k

 $\theta_k$ : phase of the received impulse on path k

 $t_k$ : arrival time of the received impulse on path k

In addition to the above data, the raytracing engine also provides spatial information such as the azimuth and elevation angles of arrival and departure for each multipath component.

The Dirac delta function  $\delta(.)$  in Formula 2.1 is a mathematical artifice consisting of an impulse of infinite amplitude and zero width, and having an area of unity. The delta function is defined as the first derivative of the Heaviside step function  $H(x)=1/2*[1+\mathrm{sgn}(x)]$  and it has the fundamental property that

$$\int_{-\infty}^{\infty} f(x)\delta(x-a) \, \mathrm{d}x = f(a) \tag{2.2}$$

From an impulse response h(t), the received signal y(t) (for an omnidirectional antenna) in response to the transmitted signal s(t) can be found as:

$$y(t) = \int_{-\infty}^{\infty} s(\tau)h(t-\tau) dx + n(t)$$
 (2.3)

where n(t) is the additive noise at the receiver (e.g. thermal noise).

In order to generate an SPS, the impulse response provided by the raytracing engine can be used to calculate the received signal strength. Two different methods to calculate the power are used in this context:

Vector Sum: 
$$P_v = \left| \sum_{k=1}^{N} a_k e^{j\theta_k} \right|^2$$
 (2.4)

Magnitude Sum: 
$$P_m = \sum_{k=1}^{N} a_k^2$$
 (2.5)

The vector sum method is the exact way to calculate the received power at a specific coordinate. Depending on the phase of various impulse components, their superposition might have destructive or constructive effects on the received power. Adding up all the impulse vectors may result in very different powers at positions, which are spatially close. This results in the fast fading phenomenon previously discussed in Section 1.5.1.

The magnitude sum method does not take any signal superposition into consideration and therefore leads to an averaged power. The magnitude sum method is equivalent to a spatially smoothed signal strength, which can be obtained by calculating the mean value of several RSS measurements in a small vicinity (such as a circular area with a radius of half the signal's wavelength). It has been shown that the magnitude sum is a good approximation of circular and linear spatial averaging of power measurements, which are subject to multipath interference (24).

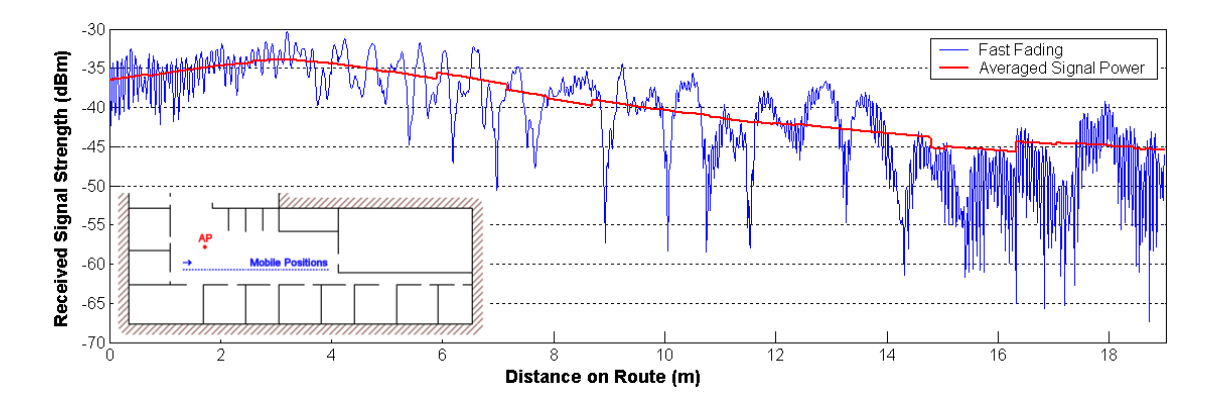


Figure 2.6: Illustration of fast fading.

Figure 2.6 visualizes the difference between the two above mentioned power calculation methods. The small building layout in the lower left corner shows the raytracing experiment setup. An access point is placed within a big hallway and a mobile device moves along a straight route, measuring the received signal power at a step size of 2 cm. The jagged blue graph has been obtained by the vector sum method, it clearly shows the effects of multipath fading. The thick red line is the average received signal strength, calculated as a magnitude sum.

#### 2.3 Beamforming

Beamforming is the combination of radio signals from a set of small non-directional antennas to simulate a directional antenna. By assembling a number of antenna elements to form an array, the direction of the main beam (its directivity) can be controlled. This is accomplished through the adjustment of the received signal amplitude and phase of each antenna element in the array. Accurate pointing of the beam in the desired direction minimizes radiation (or reception) in the unwanted directions, and it improves the signal-to-noise ratio and the overall efficiency of a wireless system. A good introduction to beamforming can be found in (11).

Array antennas with various shapes and forms (e.g. linear, circular or even spherical) find more commercial applications everyday. Linear arrays have the disadvantage that their field of view is limited to 180°. Circular arrays on the other hand allow for a full 360° beam orientation; and are therefore perfectly suited for two-dimensional positioning applications. In a circular array, the antenna is able to create a beam in one desired direction, for example the direction of the transmitter. Because of the different positions of the array elements, a narrow band signal such as  $s(t) = cos(2\pi ft + \phi)$  coming from a given direction will arrive at different times  $t_0$  and  $t_1$  at the elements (see Figure 2.7). From the antenna's point of view, this translates to different phases  $\phi_0$  and  $\phi_1$ .

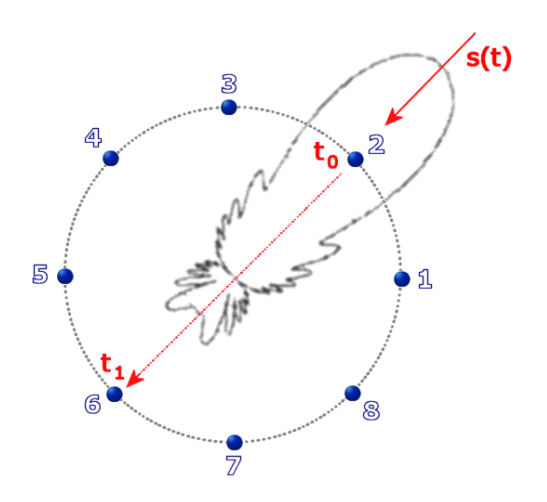


Figure 2.7: Beamforming using a circular antenna with eight elements.

The fundamental idea in beamforming is to electronically compensate the phase discrepancies of the signals at each element, such that the array can collectively amplify the received signal from a desired direction. Analogously, signals from unwanted directions can be controlled to be out of phase and therefore destroy

each other by superposition. This means that there will be severe attenuation for that direction. Combined amplitude and phase control can be used to further minimize the side lobes and to achieve a performance close to an ideal antenna.

The implementation of the beamforming algorithm used in this thesis is listed in Appendix A.1. It is coded as a MATLAB function, which takes arguments such as the number of elements and the desired azimuth of the main lobe and returns the horizontal antenna gain pattern of a circular beamformer. The raytracing engine WiSE allows gain patterns to be applied to transmitter and receiver antennas. Figure 2.8 shows the gain pattern of a transmitter with a circular array using the implemented beamforming algorithm.

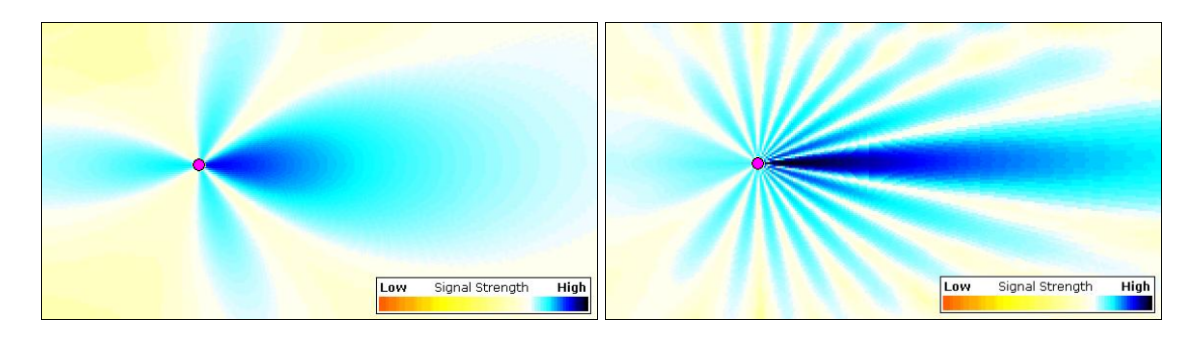


Figure 2.8: Gain patterns of circular array antennas with 4 and 32 elements, respectively.

A circular array with a beamforming capability can be used to derive spatial power spectra at the receiver coordinate. The received signal strength in general is a function of the array's gain pattern. For a given building layout, transmitter-receiver location, transmit power, frequency, and array size, the spatial spectrum at the receiver coordinates can be obtained by rotating the main lobe around the 360° field of view.

In order to further verify the accuracy of the obtained spatial spectra, a real experiment was conducted to compare sample measurements to the predicted values of the raytracing tool (See Section 2.4 for more details).

#### 2.4 Experimental Verification Of SPS

In order to justify the use of a raytracing engine for performance analyses of the SPS-based approach, verification of the accuracy of the simulated spatial power spectrum with real measurements was necessary. Therefore, an experiment was set up that involved a directional antenna located on a mechanically rotating platform (see Figure 2.9). This test was carried out with help of the Electromagnetics Division of NIST located in Boulder, Colorado.



Figure 2.9: Logarithmic periodic receiver antenna (left) and directional transmitter antenna (right)

The floorplan, which consists of two rooms, connected by an approximately 20 meter long corridor, is shown in Figure 2.10. The transmitter (also directional) is located in the smaller room in the east, faces the hallway and emits signals with a power of 40 dBm. Two different positions were selected for the receiver. These positions, which are 30 cm apart, are not in the line of sight of the transmitter. Since the building layout is located underground, the dielectric properties of the walls have been modeled as being impervious to RF signals (i.e. the attenuation factor of the walls was set to -200 dB).

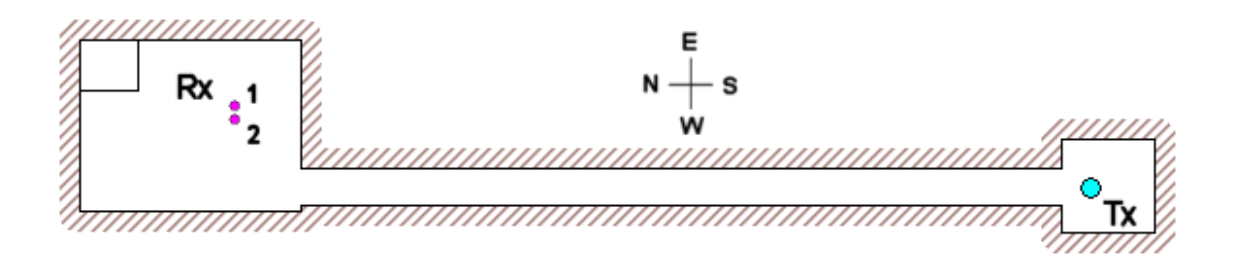


Figure 2.10: WiSE layout of the basement at NIST (Boulder, CO)

The raytracing model incorporates the antenna patterns displayed in Figure 2.11 for both the receiver and transmitter, which have been obtained from the corresponding manufacturers.

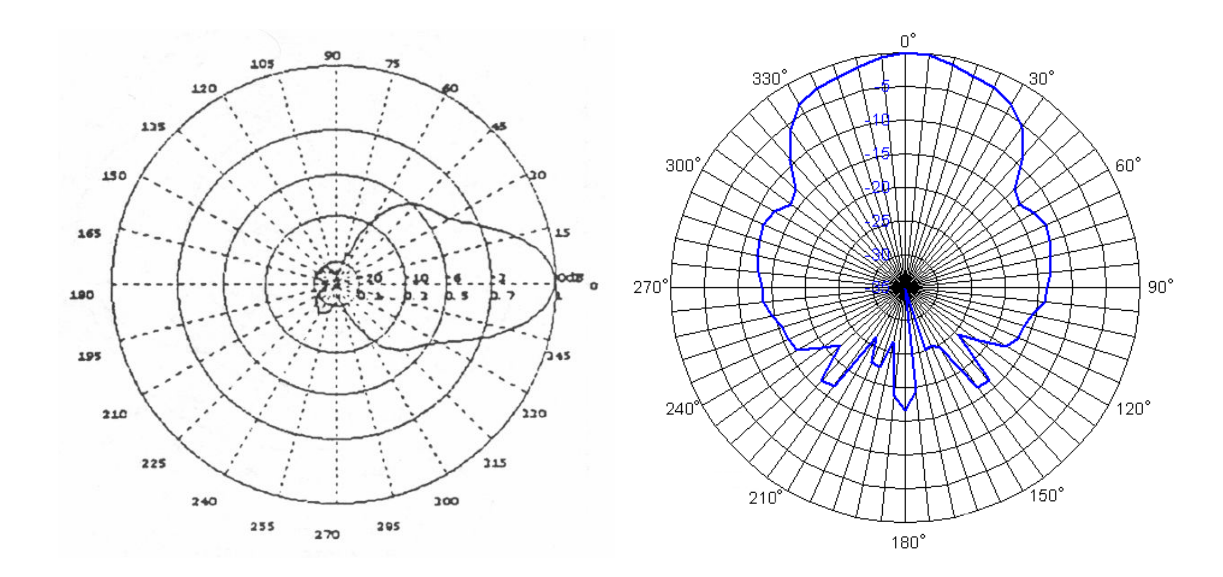


Figure 2.11: Antenna patterns of transmitter (left) and receiver (right) at 4.95GHz.

Figure 2.12 demonstrates the comparison made between the measured SPS and the simulation estimate obtained by the raytracing tool. The simulation results have been calculated with the magnitude sum method, which is the reason for their smooth behavior. On the other hand, the measured SPS plots correspond to a single physical coordinate and therefore exhibit the effects of multipath fading.

In the experiment, the SPS were generated by taking the measurement of the received power when the azimuth angle of the directional receiver antenna was pointing at  $\theta=0,10,20,...,350$  degrees. Even though they do not precisely match, both the measurement and the simulation results are following the same general pattern, which is also intuitively explainable.

- The peak seen at about 60° azimuth is caused by signals escaping the tunnel, either reflecting off the corridor walls or diffracting around the corner close to the receiver positions.
- The substantial decrease in signal strength around 100° is due to the fact that
  any signal arriving at the receiver from the wall in the west must have experienced many reflections or other considerable attenuation from scattering.
- The peak at about 170° is obviously an effect of reflections at the building's northern wall.
- Between the azimuth angles of 240° and 310° the phenomenon of fast fading is clearly visible. Except from a huge decrease in signal intensity the measurements only agree with the simulation results to a certain degree. This is caused by the scattering effect, because the corresponding area of the room is furnished with two metal desks, big wooden boxes, and other items that cause the transmitted signal to disperse in various directions.

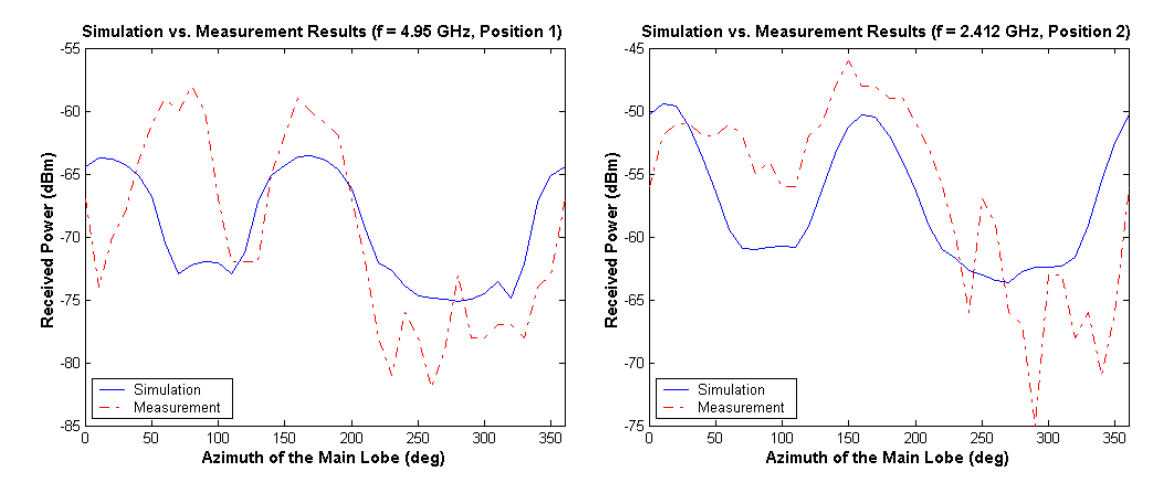


Figure 2.12: Comparing simulated spatial power spectra to data obtained from real measurements.

Aside from the justification that raytracing is well suited for studying SPS-based localization techniques, there was another important assumption that needed to be clarified, as well. In order for a localization algorithm to calculate a meaningful distance between two SPS, points close to each other in physical space must result in similar spatial power spectra. If this is the case, it would make sense to also infer physical proximity from SPS that look alike, and to use them as signatures for radio map based localization. Figure 2.13 shows two SPS, taken at positions which are 30 cm apart. It is visible that the curves closely relate, even if the distance between the two points is 5 times the wavelength of  $\lambda = 6.1$  cm.

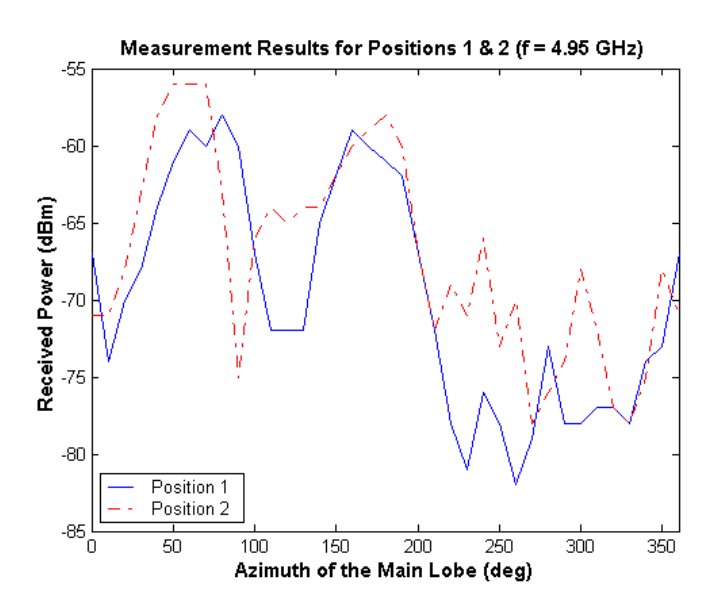


Figure 2.13: Spatial power Spectra of two physically close positions.

By averaging the sample SPS corresponding to a few nearly co-located positions, a closer match to the smoothed outcome of the raytracing tool was observed. As Section 4.4 will explain, the more points are used for averaging, the smoother the curve, and the closer it becomes to an SPS created using the magnitude sum method.

# 3 Simulation Platform

#### 3.1 General Overview

The block diagram shown in Figure 3.1 describes the simulation platform that was programmed with MATLAB in order to assess the performance of localization techniques based on spatial power spectra.

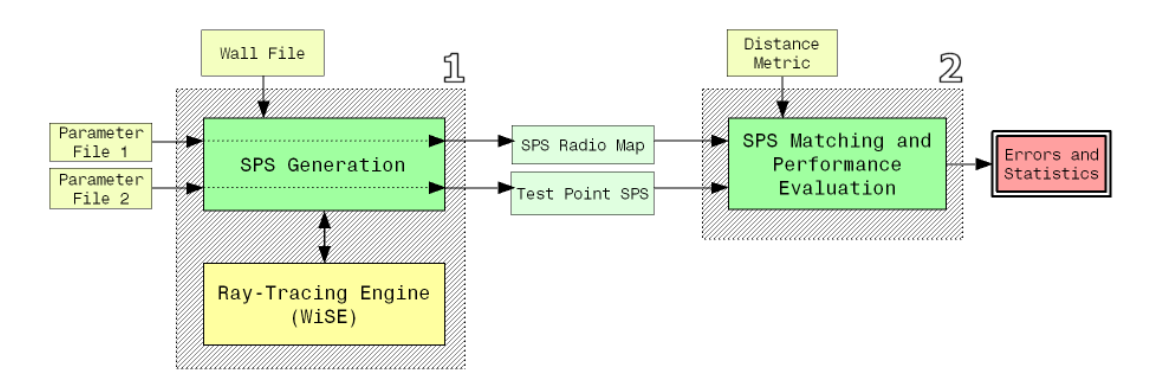


Figure 3.1: Block diagram of the simulation platform

The simulation environment consists of two main parts, which emulate the training and real-time localization phases. As a first step, a radio map containing SPS has to be built through interaction with the raytracing engine. Also, a collection of sample SPS (test points) needs to be assembled. In the second step, these outputs are then analyzed by the performance evaluation module, which employs the matching techniques and returns the error statistics.

### 3.2 Input Parameters

Performance statistics can be obtained for a multitude of input parameters, which have to be specified in a text file as shown in Appendix B.1. They can be categorized as follows:

**Raytracing Parameters** Specifications, such as the type of propagation model and the number of reflections or diffractions to use for the generation of rays, are directly forwarded to WiSE by the SPS generation process.

**Grid Parameters** The grid parameters define the locations of all the entries in the radio map. These locations are generated automatically as a layout-spanning grid with resolution  $\mathrm{d}x$  by  $\mathrm{d}y$ . A slightly different set of parameters (such as the number of random test points) is used in case of creating a collection of SPS samples; the simulation platform also allows for user defined grids.

Access Point Parameters These parameters define the number and location of access points, their center frequency and radiation power. Also, the beamforming antenna to be used for generating radio maps has to be defined by its number of array elements, the element spacing fraction and an angular rotation increment.

**Power Calculation Parameters** It is possible to calculate spatial power spectra using either the vector or magnitude sum methods previously discussed in Section 2.2. If the vector sum mode is chosen, two additional parameters (number of points and a radius) have to be specified, which define a circularly arranged set of points around the corresponding location, used for spatial smoothing.

**Building Layout** The floorplan, including the dielectric properties of the walls, has to be defined in a separate file. The format is shown in Appendix B.5.

### 3.3 Building The Radio Map

Figure 3.2 depicts the functionality of the gray shaded block 1 in Figure 3.1, which represents the training phase. It is responsible for creating radio maps.

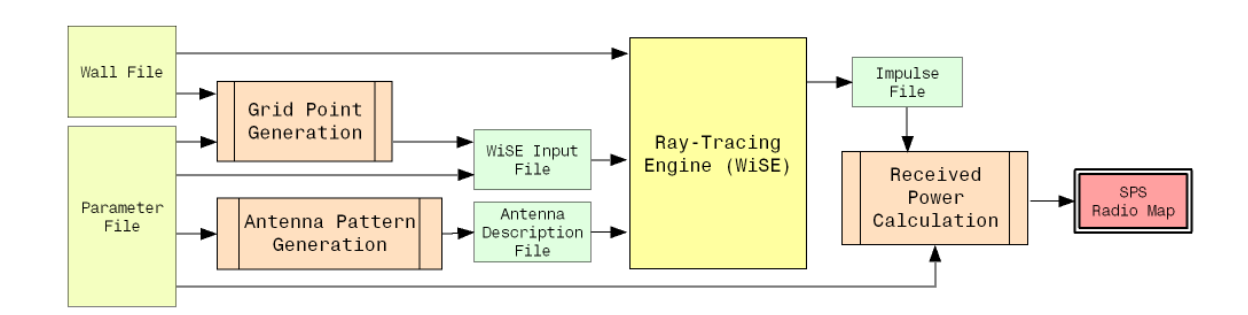


Figure 3.2: The process of creating radio maps

In favor of improved clarity, the iterative and nested nature of the radio map generation has been abstracted from the flow chart.

### 3.3.1 Definition Of The Datastructures

A spatial power spectra is implemented as a matrix with N rows and k columns, where

N: number of access points on the layout.

k: number of antenna rotation steps per 360°.

Every matrix element represents the received signal strength obtained from the access point  $AP_{i,\ i\in\{1,\dots,N\}}$  with its antenna beam directed toward azimuth  $\theta_{i,\ i\in\{1,\dots,k\}}$ :

$$SPS = \begin{bmatrix} RSS_{AP_1\theta_1} & RSS_{AP_1\theta_2} & \dots & RSS_{AP_1\theta_k} \\ RSS_{AP_2\theta_1} & RSS_{AP_2\theta_2} & \dots & RSS_{AP_2\theta_k} \\ \dots & \dots & \dots & \dots & \dots \\ RSS_{AP_N\theta_1} & RSS_{AP_N\theta_2} & \dots & RSS_{AP_N\theta_k} \end{bmatrix}$$
(3.1)

A radio map is created from a grid of size  $m \times n$  and is implemented as a matrix of the same size:

$$RADIOMAP = \begin{bmatrix} SPS_{x_1y_1} & SPS_{x_1y_2} & \dots & SPS_{x_1y_n} \\ SPS_{x_2y_1} & SPS_{x_2y_2} & \dots & SPS_{x_2y_n} \\ \dots & \dots & \dots & \dots & \dots \\ SPS_{x_my_1} & SPS_{x_my_2} & \dots & SPS_{x_my_n} \end{bmatrix}$$
(3.2)

For grid points with invalid coordinates, such as points which lie too close to a wall or fall out of the building boundaries, the radio map contains an empty entry. This might cause some overhead, but it ensures a topographically correct and easily searchable representation.

Both structures store additional data, which is important at the implementation level. For instance, each entry in the radio map contains coordinate information about the location where it has been created. A radio map includes even more data, such as the locations of the access points, the applied raytracing parameters, and also the entire building layout (for the possibility of visual representation).

The following subsections explain the different steps in the procedure of constructing radio maps.

### 3.3.2 Grid Point Generation

Initially, both the parameter file and the WiSE wall definition file are read. From the data in the wall file it is possible to extract the polygon of the outer building walls. This polygon defines the area in which radio map points are allowed to be placed. The parameter file also contains a value for the minimum distance from the walls; it is used to preserve the possibility of future practical implementation by preventing grid points from being placed too close to walls, or even inside

of them. User defined and random placements of test point coordinates can also be specified. This is useful for allocating coordinates to mobile devices, for instance to create a collection of SPS samples used in the performance evaluation. In the process of building a complete radio map, an SPS has to be generated at every grid coordinate.

#### 3.3.3 Antenna Pattern Generation

Each SPS in the radio map is created by rotating the main beam of the circular array in its 360° field of view, using a beamforming algorithm. This is done according to the rotation step size defined in the parameter file. For every azimuth which the main lobe is pointing at, a different antenna pattern has to be obtained from the function BF\_UCA\_H\_Pattern(), shown in Appendix A.1. The antenna pattern is then converted to the file format accepted by WiSE (details in Appendix B.4).

### 3.3.4 Interaction With Raytracing Engine

After the antenna description file for the current azimuth has been written, it can be passed on to WiSE, along with all the necessary raytracing parameters. These are collectively defined in a dedicated *WiSE input file* (see Appendix B.2 for format definition). The WiSE input file has to be updated for every single raytracing study, in order to incorporate the current transmitter/receiver coordinates and the name of the antenna pattern file. Additionally, a layout may contain numerous access points; a signal strength value has to be calculated for each of them. Depending on the propagation model parameters and the number of walls in the layout, it takes WiSE from a fraction of a second to several minutes to complete a raytracing study and to produce an *impulse file*. This file contains the impulse response as mentioned in Section 2.2, providing all the necessary values for the power calculation. The exact file format is shown in Appendix B.3.

### 3.3.5 Received Power Calculation

In the last step of building a radio map, the received signal strength for the current parameters has to be calculated from the impulse response that WiSE provides. If a magnitude sum calculation has been chosen, Formula 2.5 is applied and the resulting SPS is entered into the radio map. In case of a vector sum calculation, two additional parameters come into play which are used for spatial averaging. The first parameter, vs\_points, specifies the number of sample SPS to be averaged, and vs\_radius defines the circle on which they are taken. So, instead of just conducting a single simulation at the grid point's coordinates, many SPS are created around that point and then averaged by calculating the mean values per azimuth.

### 3.4 SPS Matching And Performance Evaluation

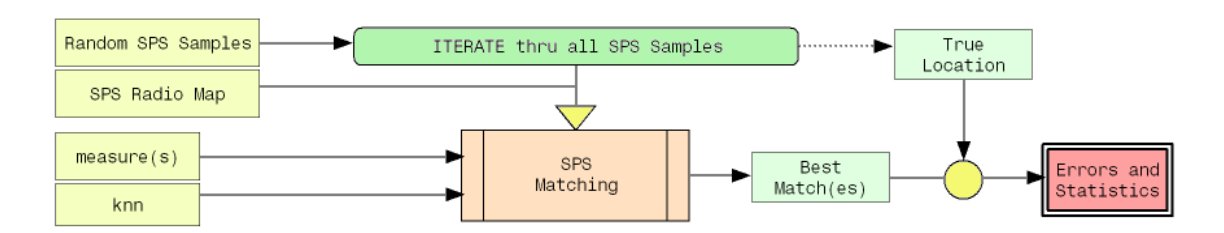


Figure 3.3: SPS Matching And Performance Evaluation

The shaded block 2 in Figure 3.1 describes the performance evaluation process for SPS-based localization. The two main inputs are a radio map and a collection of SPS samples (i.e. test points), which have both been created in the first phase. In the performance evaluation, the position corresponding to a given sample SPS is estimated, and the Euclidean distance of error between the estimated coordinates and the true position is calculated. In other words: every sample SPS is compared to all elements in the radio map, the coordinates of the best matching entry are chosen as a position estimate and the deviation from the true location is added to the error statistics.

An additional parameter knn (i.e. k nearest neighbors) can also be specified in order to return the best k matches, instead of just a single one. This might be interesting for coordinate averaging or other post-processing strategies, such as finding clusters of promising locations.

In order to compare the spatial signature of a test point to those included in the radio map, various distance measures can be used. It is also possible to use a *multi-pass* approach, which is a combination of two or more distance measures. The evaluated measures are described in the next section.

### 3.5 Distance Measures

As mentioned before, to compare the signature of a test point to those included in the radio map a distance metric needs to be defined. The following subsections describe different methods of comparing two SPS.

### 3.5.1 Minkowski Distance

Minkowski metrics are a family of distance measures, which are generalized from the Euclidean distance formula. They are often used as a similarity measure between two patterns that could be images, graphs, signatures or vectors. If  $d_{L_r}(SPS_1,SPS_2)$  denotes the distance between two signatures  $SPS_1$  and  $SPS_2$ , then the Minkowski distance of order r is defined as

$$d_{L_r}(SPS_1, SPS_2) = \left(\sum_{\theta} |SPS_1(\theta) - SPS_2(\theta)|^r\right)^{\frac{1}{r}}$$
(3.3)

where  $\theta$  denotes the angular position in the 360° field of view. At r=2, this metric is the typical Euclidean distance that has been used for some of the RSS-based methodologies (2). The performance of  $L_1$  and  $L_2$  distance metrics will be investigated for the spatial spectrum matching, as well. These metrics essentially perform an element-by-element similarity measure between the two signatures  $SPS_1$  and  $SPS_2$ , which might be ineffective for signatures that are circular shifted versions of each other. This could be especially important when the grid resolution of the radio map is low.

### 3.5.2 Area Difference

Maybe the most intuitive distance measure for comparing SPS is by calculating the absolute difference of the area under both curves. Since an SPS represents the received signal strength per azimuth at a given location, the area under its curve is a notion of the total received energy at that location. The area difference is defined as

$$d_A(SPS_1, SPS_2) = \left| \sum_{\theta} SPS_1(\theta) - \sum_{\theta} SPS_2(\theta) \right|$$
 (3.4)

By reducing a spatial spectrum to a single number, all directional information gets lost. This is an obvious disadvantage; using  $d_A$  basically causes an SPS-based algorithm to degenerate to an RSS-based method.

### 3.5.3 Kullback-Leibler Distance

From the information theory point of view, the Kullback-Leibler distance (also called *relative entropy*) has the property that it measures how inefficient on average it would be to code one SPS using the other as the code book. While  $d_{KL}$  is often called a distance, it is not a true metric because it is not symmetric and does not satisfy the triangle inequality. The Kullback-Leibler distance is defined as:

$$d_{KL}(SPS_1, SPS_2) = \sum_{\theta} \left[ SPS_1(\theta) \cdot \log \left( \frac{SPS_1(\theta)}{SPS_2(\theta)} \right) \right]$$
(3.5)

Note, that using the Kullback-Leibler distance to compare two spatial spectra is formally incorrect. SPS are not probability distributions; however, they can easily be normalized and treated as such.

### 3.5.4 Hausdorff Distance

The Hausdorff distance measures the extent to which each point on a curve lies near some point on another curve (see Figure 3.4). Or more general, the Hausdorff distance is the maximum distance of a set of points to the nearest point in another set. Thus, this distance can also be used to determine the degree of resemblance between two spatial spectra  $SPS_1$  and  $SPS_2$ :

$$d_{HD}(SPS_1, SPS_2) = \max_{\forall \theta_1} \left( \min_{\forall \theta_2} \left( \sqrt{(SPS_1(\theta_1) - SPS_2(\theta_2))^2 + (\theta_1 - \theta_2)^2} \right) \right)$$
(3.6)

The Hausdorff distance is not symmetric, but if the maximum of both possibilities is calculated, a correct metric can be obtained:

$$d_{HD}^* = \max(d_{HD}(SPS_1, SPS_2), d_{HD}(SPS_2, SPS_1))$$
(3.7)

Another disadvantage is that the Hausdorff distance only takes into account the sets of points on both curves and does not reflect the course of the curves. In other words,  $d_{HD}$  is only suitable for functions with no ambiguity in the range space. However, an SPS is a well-defined function, therefore  $d_{HD}$  should be an appropriate measure for spatial spectra. A more elaborate version of the Hausdorff distance, which accounts for the course of both curves, is called Fréchet distance (3).

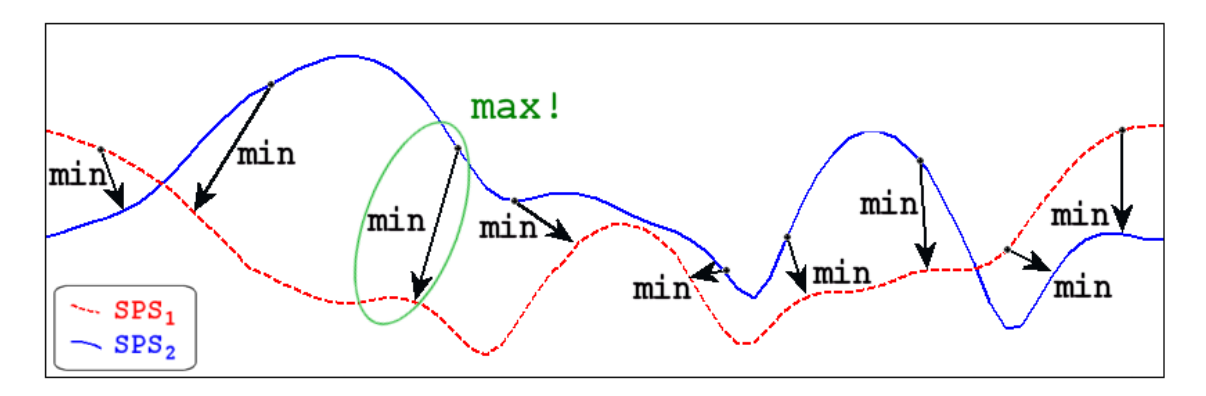


Figure 3.4: The Hausdorff distance is defined as the maximum of all minimum distances between two curves.

### 3.5.5 Earth Mover's Distance

The Earth Mover's Distance (EMD) was introduced in (21) as a distance metric with application in content-based image retrieval. An attractive property of this metric is its capability to match perceptual similarity better than other distance

metrics used for image matching. This property is actually desirable for comparing SPS as well, since in most cases perceptual matching of spatial signatures would seem to apply in coordinate matching for indoor positioning.

The EMD is based on a solution to the transportation problem from linear optimization. It is a useful and flexible distance metric which measures the minimum cost of transforming one signature into the other. Signature matching is cast as a transportation problem by defining one signature as the supplier and the other as the consumer, and by setting the cost for a supplier-consumer pair equal to the ground distance between an element in the first signature and an element on the second. Intuitively, the solution is the minimum amount of work required to transform one signature into the other. The transportation problem can be solved efficiently through linear programming. An implementation with additional MATLAB wrapper can be obtained from (20).

Alternatively, given  $SPS_1$  and  $SPS_2$ , one can be seen as a mass of earth properly spread in space, the other as a collection of holes in that same space. Then, the EMD measures the least amount of work needed to fill the holes with earth. A unit of work corresponds to transporting a unit of earth by a unit of ground distance. Or in terms of spatial spectra, a unit of work can be defined as a combination of an angular and energetical shift (as previously shown in Figures 2.3 and 2.4). It is not obvious though, how differences in signal strength and angle should be reduced to a common denominator. The basic question is: "How many units of signal strength (dB) are equivalent to an angular shift of 1°". The implementation used in the scope of this thesis uses an empirical 1 dBm  $\hat{=}$  10°, which translates to a weighing factor  $\omega=10$ . Details are displayed in Appendix A.2.

Within this document, the earth mover's distance between two spatial spectra  $SPS_1$  and  $SPS_2$  will be denoted as  $d_{EMD}(SPS_1,SPS_2)$ .

### 3.5.6 Angle Of Arrival

Instead of reducing an SPS to its total energy (as done for  $d_A$ ), it is also possible to extract the azimuth at which the most powerful measurement was observed as a comparison criterion. Given two spatial spectra  $SPS_1$  and  $SPS_2$  and their corresponding radio angles of arrival  $\theta_1 = \arg\max_{\theta}(SPS_1)$  and  $\theta_2 = \arg\max_{\theta}(SPS_2)$ , the radio angle of arrival distance measure is defined as:

$$d_{AoA}(SPS_1, SPS_2) = \min(|\theta_1 - \theta_2|, 360^\circ - |\theta_1 - \theta_2|)$$
(3.8)

For a single access point, this measure is very inaccurate, because energetically shifted SPS (see Figure 2.3) result in zero distance if compared to each other. A random SPS of those lying in the right direction would be estimated as the correct location, which would most likely result in an error of many meters. An improved

version of  $d_{AoA}$  can be obtained by also incorporating the absolute power values measured at  $\theta_1$  and  $\theta_2$ :

$$d_{AoA}^*(SPS_1, SPS_2) = \sqrt{\min(d_{AoA}(SPS_1, SPS_2)^2 + \omega \cdot (SPS_1(\theta_1) - SPS_2(\theta_2))^2}$$
 (3.9)

where  $\omega$  is the weighing factor described in the previous section.

### 3.5.7 Multi-Pass Approach

Distance measures can be combined in order to improve localization accuracy. For example,  $d_A$  could be used in a first step to find the candidate SPS which best according to received power. In a second pass, the best matching SPS could be calculated using  $d_{AoA}$  as a distance measure. The overlap of both sets would then dramatically reduce the possible locations to fall into a small region. A visualization of this technique is displayed in Figure 3.5. Radio map entries are represented by dots. A sample SPS has been taken at the indicated location. The 100 signatures that best match the sample SPS are highlighted for both the  $d_A$  (red) and  $d_{AoA}$  (blue) measures. The intersection of both sets (green) is where the mobile node must be located.

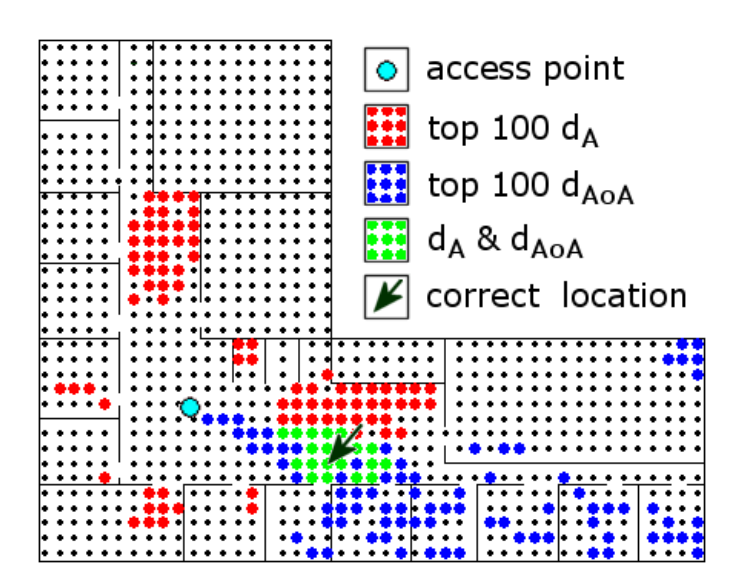


Figure 3.5: Combining two measures to further narrow down the true location of a mobile node.

One problem in combining different measures is that all the previously mentioned distance measures have completely different absolute values. For instance, the distance  $d_{L_1}(SPS_1,SPS_2)$  has no relation to  $d_{EMD}(SPS_1,SPS_2)$ . Therefore, distance values have been normalized, such that all distances of an SPS to every other SPS in a radio map sum up to 1. Internally, a ranking for the whole radio

map is kept, which can be interpreted as a probability distribution. In case of a multi-pass approach, these distributions are then multiplied, and the top entry is chosen as the best matching candidate. Figure 3.6 shows the ranking of all entries in a radio map, compared to a sample SPS, taken at the indicated location.

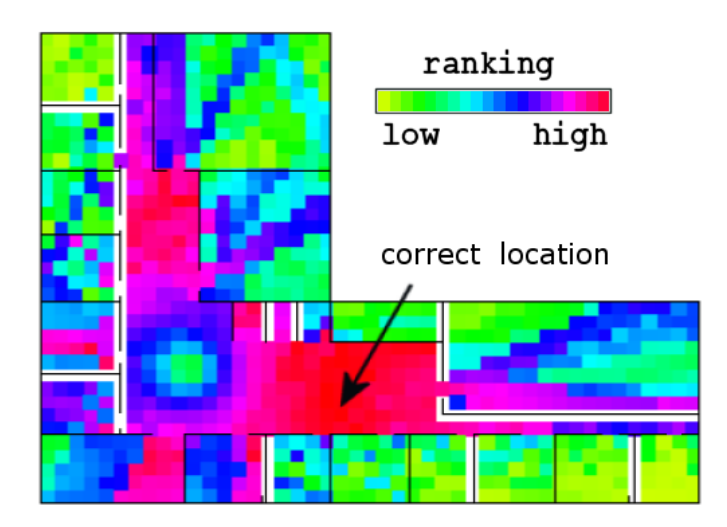


Figure 3.6: Ranked radio map entries.

# 4 System Performance

Using the simulation platform discussed in the previous section, experiments have been conducted for various antenna array sizes, radio map grid resolutions, spatial spectrum resolutions (i.e. beam rotating step sizes), signature matching techniques, and more. Due to the large number of system variables, reasonable default values have been chosen for a basic set of simulation parameters (see Table 4.1). Keeping a basic set of values fixed makes it easy to monitor the behaviour of the system as affected by the variables of interest.

Transmit power:	15 dBm
Center frequency:	2.4 GHz
Antenna heights:	1.8 m
Minimum distance to walls:	25 cm
Number of reflections:	5
Number of diffractions:	0

Table 4.1: Constant simulation parameters.

The main objective here, is to study the applicability of SPS-based localization techniques in indoor environments. In order to establish a meaningful basis for comparison and performance evaluation, a reference system was chosen that is equivalent to the RSS-based method outlined in Section 1.5.2.

Section 2.3 described how circular array antennas with beamforming capabilities are implemented. Notice that the beamforming antenna used for SPS generation can be modeled as being composed of only a single element. In this case, beamforming is not possible, and the antenna degenerates to an omnidirectional one. This essentially leads to a pure signal-strength-based system where no directional information is included in the signatures and the radio map. In this case, each spatial spectrum is replaced by a scalar that represents the total average received power. Performance of this omnidirectional system with an  $L_2$  distance metric has been chosen as the benchmark for comparison purposes.

### 4.1 Comparison Of Distances Measures

Table 4.2 summarizes the average position error<sup>1</sup> obtained with different matching algorithms, number of access points, and radio map grid resolutions. The number of array antenna elements used for the simulation results is 8, and the rotation step size (i.e. SPS resolution) was set to 5°. The first row displays the average position error of the benchmark system, which is purely based on received signal strength. Other rows give information about the average position error of the SPS-based technique, evaluated for various distance measures.

	Radio Map Res. 1m			Radio Map Res. 2m			Radio Map Res. 3m		
Measure	AP = 1	AP = 2	AP = 3	AP = 1	AP = 2	AP = 3	AP = 1	AP = 2	AP = 3
RSS ( $d_{L_2}$ )	15.8	4.37	2.50	16.0	5.54	4.32	16.4	6.66	5.53
SPS ( $d_{L_2}$ )	0.83	0.82	0.99	3.10	2.12	2.48	5.07	4.58	2.90
SPS $(d_{L_1})$	1.03	0.86	1.06	3.20	2.46	2.34	5.05	4.11	2.77
SPS ( $d_{EMD}$ )	1.05	1.18	1.02	3.22	2.28	2.59	5.95	4.49	3.07
SPS $(d_{AoA}^*)$	1.90	1.50	1.72	4.97	4.10	3.31	6.88	6.03	4.41
SPS $(d_{HD})$	2.30	1.59	2.05	5.12	3.11	3.08	7.98	4.52	3.68
SPS $(d_{KL})$	2.64	1.35	1.87	5.88	4.28	3.13	7.56	5.52	4.25
SPS ( $d_{AoA}$ )	14.7	5.4	2.99	11.9	8.00	4.94	11.4	8.89	8.51
SPS $(d_A)$	15.3	4.82	3.11	15.2	6.45	3.70	17.0	8.67	4.67

Table 4.2: Average position errors (m) for all the evaluated algorithms.

The following conclusions can be drawn from the data in Table 4.2:

- As expected, a higher radio map resolution results in more accurate positioning, no matter which distance measure is used. Figure 4.1 shows the same trend in more detail, based on a larger data set.
- SPS-based localization with a single access point, in combination with the best SPS matching algorithm, results in a position accuracy which is more than twice as high as if a pure RSS-based method with three access points is used.
- The RSS-based algorithm is unable to give meaningful localization estimates when using a single access point; it benefits greatly from an increased number of access points. On the other hand, most of the SPS-based methods already perform at their best accuracy using just a single access point.
- ullet The most sophisticated distance measure, the earth mover's distance, has localization accuracy in the order of the radio map resolution. For the studied scenarios,  $d_{EMD}$  is yet unable to outperform the Minkowski distance

<sup>&</sup>lt;sup>1</sup>Throughout this thesis, the average position error is always based on 100 randomly chosen test points.

measures  $d_{L_1}$  and  $d_{L_2}$ . It is conceivable that  $d_{EMD}$  could have some advantage for lower radio map resolutions and high numbers of antenna array elements.

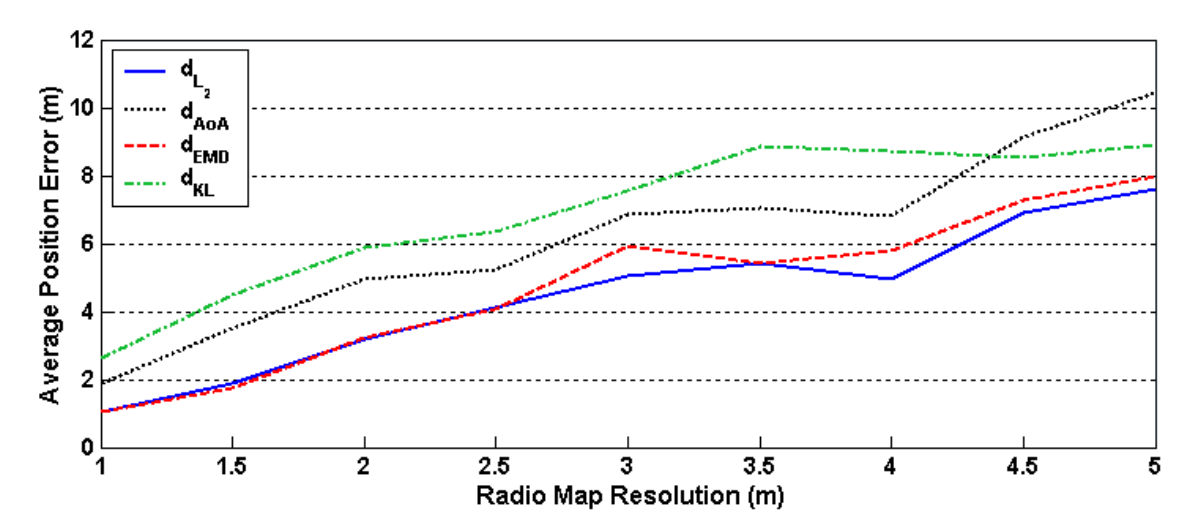


Figure 4.1: The average position error as a function of the radio map resolution, for a selected set of distance measures.

For the above results, the position of the best matching point in the radio map was selected as the estimated position of the mobile node. Selecting the best k matches and averaging the results did not amount any significant differences; therefore, those results are not listed in the table.

Table 4.3 shows the performance of SPS-based localization with combined distance measures; the results were obtained using the multi-pass approach described in Section 3.5.7. The combination of the Minkowski distance measures  $d_{L_1}$  and  $d_{L_2}$  does not amount to any noticeable improvement. Combining pure direction  $(d_{AoA})$  and range  $(d_A)$  estimates, however, reduces the position error significantly. Note that a single access point using either  $d_A$  or  $d_{AoA}$  has no localization capability at all, but jointly they yield position accuracy comparable to the RSS-based method for three access points.

	Radio Map Res. 1m		Radio Map Res. 2m			Radio Map Res. 3m			
Measure	AP = 1	AP = 2	AP = 3	AP = 1	AP = 2	AP = 3	AP = 1	AP = 2	AP = 3
$\{d_{L_1}$ , $d_{L_2}\}$	0.99	0.88	0.99	3.08	2.37	2.33	4.93	4.55	2.87
$\{d_{L_1}$ , $d_{EMD}\}$	1.05	0.82	0.99	3.17	2.09	2.50	5.12	4.32	2.91
$\{d_{AoA}, d_A\}$	2.93	2.11	1.69	6.28	4.90	3.37	9.14	6.16	3.89

Table 4.3: Average position errors (m) combining measures in a multi-pass approach.

Figure 4.2 displays the cumulative distribution function (CDF) of the error for the position estimation. In the two plots (each for a different radio map resolution),

the performance of the SPS-based method with only one access point has been compared to the performance of the RSS-based method with one, two and three access points. As observed, using the SPS approach, there is a significant improvement in accuracy when the number of access points is less than three.

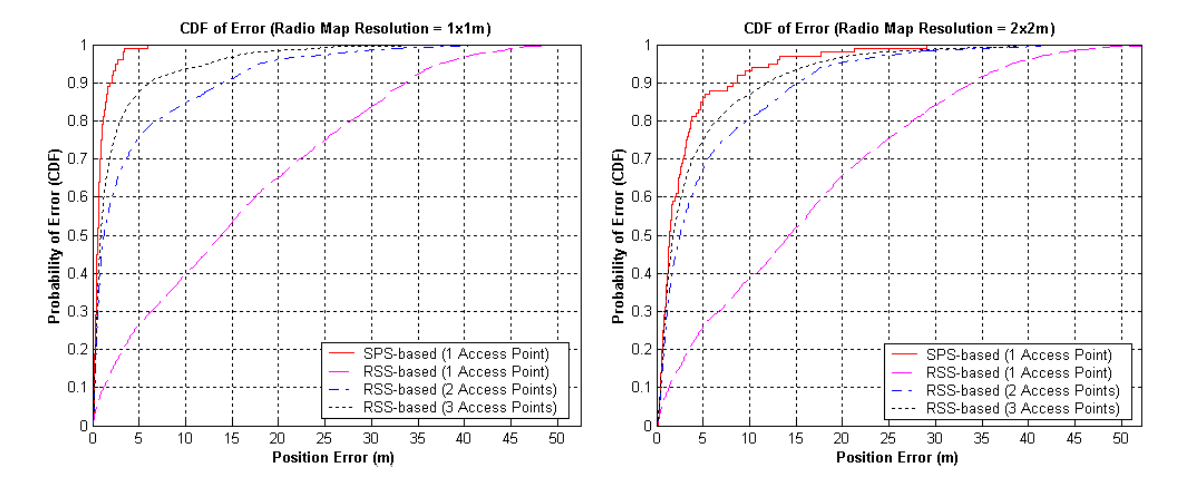


Figure 4.2: Cumulative distribution function (CDF) of the position error. The data was generated using an 8-element array antenna and a rotation step size of 5°.

Another visualization of the advantage of using spatial spectra is shown in Figure 4.3, which shows the dependency of the average position error versus the radio map resolution for low numbers of access points.

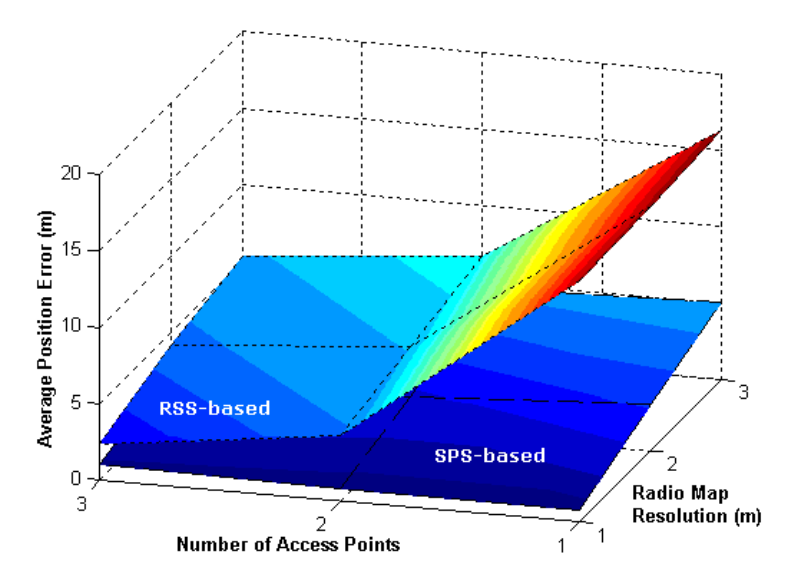


Figure 4.3: 3D visualization of the position accuracy against the radio map resolution and the number of access points.

### 4.2 Antenna Array Size

As the number of array elements increases, the main beam of the antenna becomes narrower. In the ideal case of having a needle-like beam and no side lobes, the antenna would be capable of measuring the fine-grained spatial multipath profile of the signal at the receiver location. On the other hand, an array with just one element degenerates to an omnidirectional antenna with no beamforming capabilities at all. One drawback is, that additional array elements increase the hardware complexity and costs of a beamforming antenna. Therefore it is important to study the effects of different antenna array sizes on the overall SPS-based localization performance.

Figure 4.4 shows the results of an extensive simulation, which was carried out for all possible array sizes of up to 16 elements, and for three different radio map resolutions. A single access point was deployed, which had its antenna rotation step size set to  $5^{\circ}$ . The used distance metric is  $L_2$ .

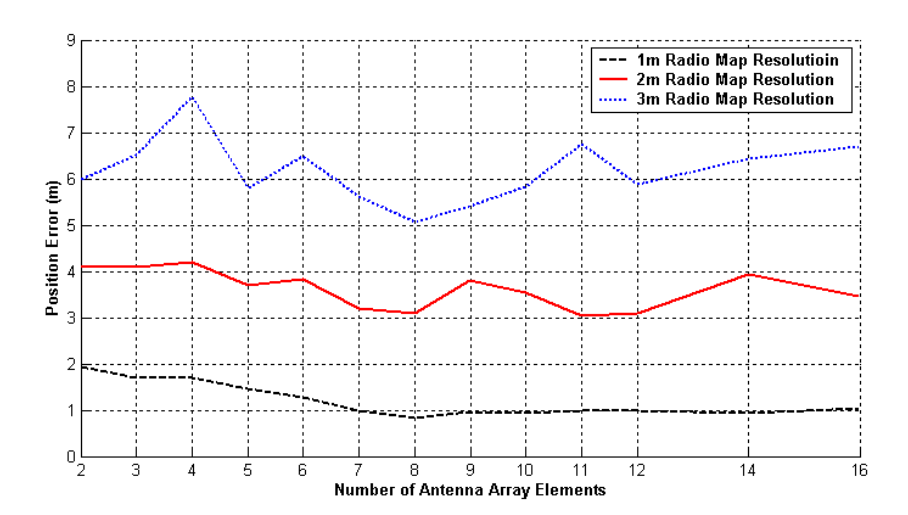


Figure 4.4: Varying the number of array antenna elements.

The number of elements in the array antenna clearly affects the average positioning error. Especially in the case of the highest tested radio map resolution (1 meter), increasing array size improves the system performance. Surprisingly, a single access point with a very low number of array elements (e.g. 2 or 3) has a localization accuracy comparable to the RSS-based benchmark method using three access points.

Initially, Figure 4.4 has been created to ascertain an optimal array size for all further studies. All three shown graphs have a local minimum at 8 array elements, which is a reasonable size for practical implementation and has therefore been chosen as a default value for the array antenna size.

### 4.3 Antenna Rotation Step Size

In order to generate an SPS, the main lobe of the array is rotated in discrete steps<sup>2</sup>, using a beamforming algorithm. Figure 4.5 shows the effect of varying the rotation step size (or SPS resolution). As expected, a general trend of increasing position error with lower SPS resolution is visible. But surprisingly, small loss in performance is observed even with large rotation step sizes (such as 45° and 90°). High SPS resolutions directly translate to more extensive radio maps. At the same time, the complexity of the SPS matching process will increase. Choosing larger step sizes for beam rotation, the computational complexity could be greatly reduced, while the localization performance would not suffer significant loss.

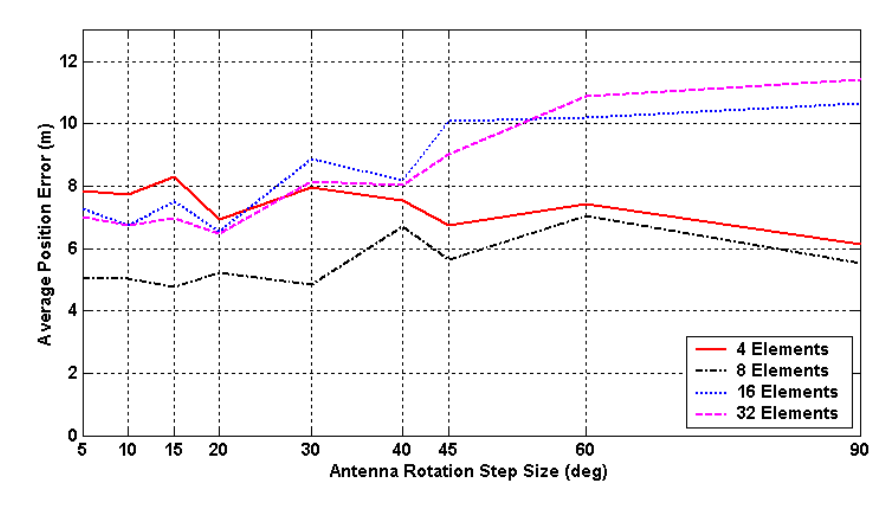


Figure 4.5: The average position error as a function of the antenna rotation step size, plotted for various antenna sizes.

It is interesting to note, that an 8-element circular array antenna with beamforming capability and a rotation step size of 45° is equivalent to a sectorized antenna with 8 sectors.

### 4.4 Magnitude Sum vs. Vector Sum

For all previously described simulations, the magnitude sum method (Formula 2.5) was used to calculate the received signal strength from the impulse response given by the raytracing engine. By using the magnitude sum method, the power values stored in the spatial power spectra are average values, which do not exhibit any multipath interference. However, measurements of any practical implementation would be affected by the fast fading phenomenon of the indoor channel; therefore, it should be investigated if the presented SPS-based ap-

<sup>&</sup>lt;sup>2</sup>It is assumed here that the rotation step size is an integer fraction of the total 360° field of view.

proach would still be able to maintain its performance under such circumstances.

Spatial smoothing is a method to achieve an averaged SPS; it is the procedure of calculating the mean value of several SPS measurements, which were conducted at positions slightly deviating from the actual location. For instance, Figure 4.6 depicts three versions of a spatial spectrum. Two of them were calculated at the same physical coordinates  $(x_0,y_0,z_0)$  with the magnitude and vector sum methods. The third one is the average of four SPS, which have been generated at positions lying on a circle around  $(x_0,y_0,z_0)$ , with a radius of 10 cm. While the multipath fading effects are clearly visible for the SPS graph calculated with the vector sum method, just four averaged samples are able to generate a curve almost congruent to the one calculated with the magnitude sum method.

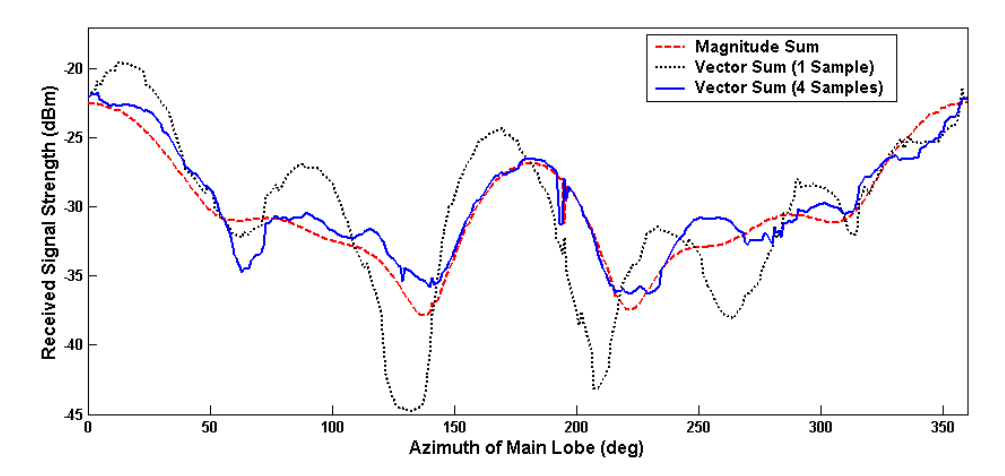


Figure 4.6: The influence of the magnitude and vector sum calculation methods on SPS plots.

Figure 4.7 shows the average error for SPS-based localization when varying the two parameters (i.e. number of points and radius) used for the vector sum method. The used radio map resolution is set to 3 meters and the layout contains one access point using an 8-element array antenna with a rotation step size of 5°. The graph in which the position error is a function of the number of sample points has been created for a fixed radius of 10 cm. Similarly, the number of points is set to 4 in the other graph.

Using no spatial smoothing definitely has a negative impact on the overall localization performance. For the studies in Figure 4.7, the position error increases from 5 to 8 meters ( $\approx$  60%) for a single SPS sample, compared to a system based on perfectly smoothed SPS. However, as the number of sample points increases, the performance approaches the level of SPS generation using the magnitude sum method. On the other hand, the radius used for placing the sample points does not seem to be a crucial factor. A radius from half up to a full wavelength of the received signal seems to be a good choice for the placement.

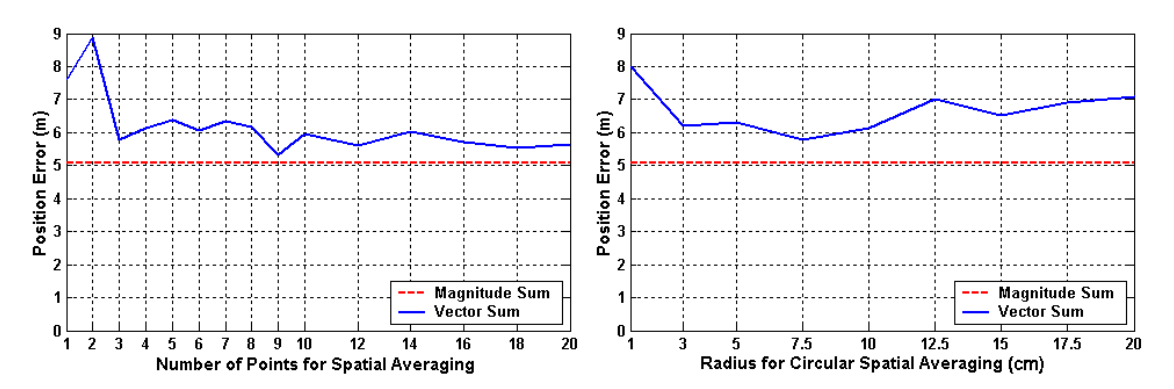


Figure 4.7: The effect of varying the number of points (left) and the radius used for circular spatial averaging (right) of SPS calculated with the vector sum method.

Pure RSS-based localization techniques are also influenced by multipath fading. It is therefore necessary to check whether vector sum calculations make any difference to an overall comparison between RSS- and SPS-based localization. Figure 4.8 shows the CDF plots of the position error for the SPS-based localization using one access point compared to RSS-based localization with up to three access points. For the spatial smoothing, 4 sample points have been chosen on a radius of 10 cm around the test locations. It is obvious that simulations using the magnitude sum are legitimate, because they can be closely approximated by spatial smoothing. It can also be concluded that the relative performance gain of SPS-based compared to RSS-based localization is still maintained in this case.

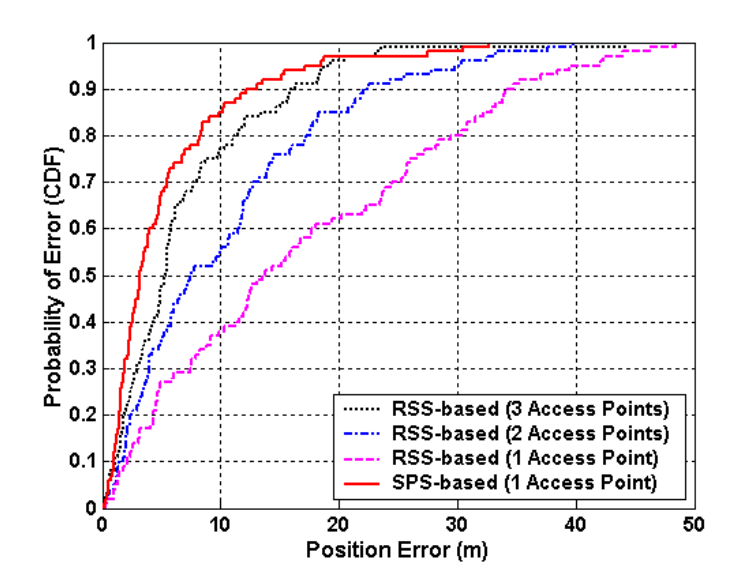


Figure 4.8: Cumulative distribution function (CDF) of the position error using the vector sum method for power calculation.

### 5 Conclusions

The underlying philosophy in this thesis is, that exploiting the information in the spatial distribution of RF energy around a receiver results in better location estimation of a mobile node. This spatial power spectrum basically represents a signature that only depends on the relative location of the transmitter-receiver pair and the environment surrounding them. It can be easily seen that in free space, there is a one-to-one correspondence between the transmitter position and the received SPS. If the receiver is assumed to be at the origin of a polar coordinate system, the received spatial signature is a function of the polar coordinate of the transmitter. If the receiver-transmitter pair is planted inside a building, the layout and the construction material of the walls dictate the flow of energy and therefore the shape of the signature. However, the uniqueness of the SPS signatures is still maintained in an indoor environment. Therefore, if a database consisting of a set of representative points (such as a radio map) in a building is made, then any inquiry to the whereabouts of a mobile device can be answered by comparing the received spatial power spectrum with the entries in the radio map.

RSS-based methodologies also follow the same strategy; however, for them to have a reasonable accuracy, radio visibility of the mobile device by at least three access points is required. This generally creates a difficult coverage design problem, which would be eliminated if SPS signatures were used instead. In other words, an advantage of using the SPS signatures as opposed to RSS (i.e. pure signal strength) is that even a single receiver with beamforming capability delivers good accuracy; and as a result, complicated triple coverage by (at least) three access points is no longer required. Theoretically speaking, if the capability of estimating both direction and range of a mobile exists, then a single access point is enough to estimate the position of any mobile transmitter. According to best knowledge, no known methodology currently exists that is capable of providing reasonable direction estimation and range information in extensive indoor environments.

Throughout all the presented simulations, only the case was considered where a stationary access point with circular array is the receiver and the mobile node is the transmitter. It is also possible to consider the case where the mobile device is the receiver capable of generating spatial signatures; however, it should be noted that in this case, the mobile receivers requires an electronic compass (or a similar device) in order to have a reference frame for azimuth angle.

### **Outlook**

The application of Multiple-In-Multiple-Out (MIMO) technology in WLAN (e.g. 802.11n) is creating the possibility to have access points that are capable of creating beam patterns which adapt to user's location. Access points that can select the best directional beam pattern among a finite number of possible patterns are already making their way into the market. It is conceivable that a simplified version of the proposed approach can be built over such infrastructure. The author hopes to implement a prototype of an SPS-based localization algorithm in the near future. One possible way could be to purchase one of the few existing array antennas that are commercially available, such as the one shown in Figure 5.1 and described in more detail online (18).

Another interesting future activity would be to reconceive SPS-based localization, but focusing on tracking, instead of stationary localization.



Figure 5.1: The Netgear RangeMax MIMO pre-802.11n wireless access point is able to configure the seven embedded circuit-board arrays into one of 127 different beam patterns.

# A Implementation Details

# A.1 Beamformer: Pattern Generator for Circular Array Antenna

The function BF\_UCA\_H\_Pattern() creates the horizontal antenna gain pattern (in dBm) for a circular beamformer. Among others, the input parameters include the number of antenna array elements and the direction of the main lobe.

```
function Sx = BF_UCA_H_Pattern(teta, freq, L, frac, dir);
% Inputs: teta: Input azimuth range of interest for antenna gain pattern [deg].
          freq: Operating frequency of the receiver [Hz].
%
                Number of antenna elements in the array.
%
          frac: Fraction of lambda for antenna elements spacing.
          dir: Direction of interest for the main lobe [deg].
% Output: Sx:
                Beamformer antenna gain pattern
P = max(size(teta, 2), size(teta, 1));
c = 299792458;
Omega = 2 * pi * freq(1);
lambda = c / freq(1);
Ant_Rad = frac * lambda / (2 * sin(pi / L));
% generate steering vectors for zero azimuth
for i = 1:L
    phi_L(i) = 2 * pi * (i - 1) / L;
    tau = -1 * Ant_Rad * cos(dir * pi / 180 - phi_L(i)) / c;
    x(i, 1) = exp(-j * Omega * tau);
end;
for k = 1:P
    for b = 1:L
        phi_L(b) = 2 * pi * (b - 1) / L;
        tau = -1 * Ant_Rad * cos(teta(k) * pi / 180 - phi_L(b)) / c;
        a(b, 1) = exp(-j * Omega * tau);
    end
    Sx(k) = 10 * log10(abs(a' * (x * x') * a));
end;
```

### A.2 Earth Mover's Distance

The function emd() calculates the earth mover's distance between two given spatial power spectra. It uses the MATLAB wrapper emd\_wrapper() (available at (20)) to solve the transportation problem.

```
function dist = emd(SPS1, SPS2);
  dist = 0;
  SPS1 = abs(SPS1); SPS2 = abs(SPS2);
                                        % because dB values are negative
  n = size(SPS1, 2);
                                        % number of angles per SPS
  step\_size = 360 / n;
  for ap = 1:size(SPS1, 1)
                                        % iterate through all access points
      DEMAND = SPS1(ap, :);
      SUPPLY = SPS2(ap, :);
      DIST = [];
                                        \% create the distance matrix
      for s = 1:n;
          for d = 1:n;
              dy = SUPPLY(s) - DEMAND(d);
              dx = min(abs(s - d), n - abs(s - d)) * step_size / 10;
              DIST(s, d) = sqrt(dx ^2 + dy ^2);
          end;
      end;
      dist = dist + emd_wrapper(DIST, SUPPLY, DEMAND);
  end
```

### A.3 List Of Functions

The following tables list the MATLAB functions implemented for the simulation platform, which was used for performance evaluation of SPS-based localization.

### **Core Functions**

Function	Description
buildSPSradiomap()	Builds a radio map from a given parameter file, using
	an interface to WiSE in order to generate spatial power
	spectra.
nearestSPS()	Finds the radio map entry closest to an SPS, using a
	given distance measure.
calcSPSerrors()	Calculates error statistics for a collection of sample SPS
	for a given radio map and distance measure.
readimpulsefile()	Reads the text file where WiSE stores the impulse re-
	sponse of a raytracing study.
calcrecvpow()	Calculates the received signal strength from an im-
	pulse response with either the magnitude or vector
	sum method.
readwisefloorplan()	Reads the wall file format of WiSE and extracts the
	outer building polygon.
BF_UCA_H_Pattern()	Creates the horizontal antenna gain pattern for a cir-
	cular beamformer.
<pre>xygridfromfloorplan()</pre>	Creates a grid of points over a given floorplan.

Table A.1: Core Functions: SPS generation and error calculation.

### Visualization and Displaying Radio Maps

Function	Description
plotSPSradiomap()	Visually displays a radio map as a combination of the
	floorplan and the grid points, including the coverage
	areas of all access points.
plotfloorplan()	Plots the wall segments of a floorplan.
plotnearest()	Displays the $k$ SPS within a radio map, which best
	match a given SPS.
plotgrid()	Plots a radio map as a grid of points.
createSPSmovie()	Creates an AVI movie of SPS plots from a given se-
	quence.

Table A.2: Visualization Functions.

### **Auxiliary Functions**

Function	Description	
calcarray_UCA()	Returns the coordinates of a number of points around	
	a specified point, lying on a circle with given radius .	
cellcell2num()	Converts a cell array of a cell array of numbers to a	
	matrix.	
createantennafile()	Converts an antenna gain pattern obtained by	
	BF_UCA_H_Pattern() to the format used by WiSE.	
coverageareas()	Calculates the coverage areas of access points in a	
	radio map as the convex hull of the points above a	
	given receiver sensitivity.	
num2zeroinfrontstr()	Returns numbers as strings with padded zeros in front.	
<pre>pointlinesegdist()</pre>	Calculates the distance from a point to a line seg-	
	ment.	
readtokenfile()	Reads text files as a collection of lines of tokens, using	
	the tokenize() function to convert text lines to tokens.	
reduceSPSangles()	Artificially reduces the size of an SPS, in order to simulating	
	late smaller rotation step sizes.	
sensitivityfilter()	Sets all values in an SPS to the given receiver sensitivity,	
	in case they are below the receiver sensitivity.	
shiftcols()	Circularly shifts the columns of a matrix by a specified	
	number of columns.	
tokenize()	Splits a string into tokens and returns them as a cell	
	array.	
tok2str()	Converts a cell array of tokens, created by tokenize()	
	back to a string.	
wiseparget()	Returns parameter lines with a given name from read	
	token files.	
wiseparset()	Changes values in a collection of tokens read by	
	readtokenfile().	
writetokenfile()	Writes a collection of tokens which have been read by	
	readtokenfile() or created by tokenize() into a text	
	file.	

Table A.3: Utility functions used by the main programs.

### **B** File Formats

### **B.1** Parameter File Format

The following code is an example of an input parameter file, used for the generation of radio maps and sample spatial power spectra. The order of the lines is not important.

```
prediction image 2
                         % Name of propagation model
nbounce 5
                         % Number of reflections
betasmin 0.01
                         % Ray pruning factor
sum_mode 0
                         % Vector sum = 0, magnitude sum = 1
                         % Number of points for averaging
vs_points 7
                         % Radius for averaging circle [m]
vs_radius 0.1
                         % Grid = 0, random = 1, user = 2
grid_mode 2
dx 1
                         % Grid spacing (x-axis) [m]
dy 1
                         % Grid spacing (y-axis) [m]
mindist 0.25
                         % Minimum allowed distance to walls [m]
rand_n 100
                         % Number of random points
AP 35 -60 1.8 2.4 32
                         % List of Access Points [x y z freq power]
AP 50 -46 1.8 2.4 32
                         % Frequency: [GHz], power: [mW]
AP 50 -60 1.8 2.4 32
elem 8
                         % Number of array antenna elements
turn_step 5
                         % Angular rotation increment of antenna
frac 0.4
                         % Fraction of lambda for antenna elements spacing.
mob_z 1.8
                         % Height of mobile [m]
                         % Grid coordinates in user mode (grid_mode 2)
MOB 25.5118 -50.3324
MOB 37.5689 -67.8108
MOB 28.8110 -44.9939
MOB 43.1022 -32.9193
MOB 31.1855 -34.2634
```

### **B.2 WiSE Input File Format**

The WiSE input file contains all simulation parameters needed by the raytracing engine. Aside from raytracing-specific values, the transmitters (xmit) and receivers (rcvr) are also defined in this file; as lines of keyword/value pairs. Their exact format is:

[xmit|rcvr] index x y z {power mw} {antenna type} {azimuth degrees} {tilt degrees}

Here is an example of a complete WiSE input file:

```
filetype bounce
output impulse
statusfile C:/wise21/b.stat
title "Example WiSE Input File"
prediction image 2
nbounce 1
ndiffract 0
betasmin 0.01
power 34 0
freq 1.92 1.920
threshold -70
reception simulcast
summation magnitude
polarization 0
rayspacing 10
raythreshold 1.0E-15
rayangle 2
coaxcouplingloss 60
coaxattenuation 0.1
coaxlossdist 2
xmit 1 7.04 12.7 3.0 power 34 azimuth 0 tilt 0 antenna isotropic
xmit 2 19.5 4.81 3.0 power 34 azimuth 0 tilt 0 antenna BF_elem04
xmit 3 16.9 12.5 3.0 power 34 azimuth 0 tilt 0 antenna BF_elem08
rcvr 1 8.23 11.3 1.0 power 0 azimuth 0 tilt 0 antenna isotropic
```

### **B.3 WiSE Impulse File Format**

The WiSE impulse file stores impulse response data generated by the raytracing engine. The file contains a block of ray data for each transmitter/receiver pair. To delimit blocks of multipath components, lines are used of the format:

```
impulse xmit_index rcvr_index #rays
```

For each multipath component, the following data is provided (where az stands for azimuth and el for elevation):

ray\_index magnitude(V) phase(°) delay(ns) xmit\_az xmit\_el rcvr\_az rcvr\_el

The following impulse file was created from the example parameter specifications in Appendix B.2, using a floorplan which is not shown here.

```
impulse 1 1 4
0 0.0088359  3.14843  9.03632  -49.2679 137.585 -49.2679 137.585
1 0.0060981  118.907  10.7128  61.6166 128.569 -61.6612 128.528
2 0.0026626  16.6182  12.6233  -49.2679 28.9078 -49.2679 151.120
3 0.0019668 -79.0462  24.3922  -80.2383 105.876  80.2371 105.878
impulse 2 1 1
0 0.0025891 -153.458  58.4804  21.9204 96.5527 158.086 96.5508
impulse 3 1 4
0 0.0026344 -69.0477  30.0339  -171.941 102.834 -171.941 102.834
1 0.0116894 -115.592  30.7808  164.843 102.519 -164.782 102.518
2 0.0031699 -112.324  37.9556  -173.691 100.124 -6.31317 100.131
3 0.0029241 -89.7315  62.9861  -3.75908 96.0812 -176.241 96.0804
```

### **B.4 WiSE Antenna Definition File Format**

WiSE uses an interpolation scheme to approximate the 3-dimensional pattern of an antenna, whose gain in two perpendicular planes is given in an antenna description file. The header of this file describes the antenna in words and is not used for the raytracing process. The body of an antenna file consists of three parts, which define the gain patterns of the horizontal plane, the vertical front lobe and the vertical back lobe. The gain function represents the gain in dB in a particular direction, so a null in the radiation field corresponds to a gain of  $-\infty$  dB. Lines such as <code>|HORIZ|s|n|</code> start a new plane with known gain values at n angles, beginning at s degrees.

```
|MANUF|Schwarzbeck Mess-Elektronik|

|MODEL|VULP 9118-C|

|DESCR|Logarithmic-Periodic Test Antenna|

|HORIZ BEAM WIDTH|360|

|VERT BEAM WIDTH|180|
```

Table B.1: The WiSE antenna file header.

HORIZ 0 24	VERT 0 12	VERT 180 12
0  -0.0	-90 -15.0	-90 -15.0
15  -0.7	-75  -8.0	-75 -20.0
30  -2.0	-60  -4.0	-60 -22.0
315  -7.0	60  -2.2	60 -14.0
330  -2.0	75  -5.2	75 -11.0
345  -0.7	90  -7.8	90  -7.8

Table B.2: The WiSE antenna file body: horizontal and vertical gain patterns.

### **B.5 WiSE Wall File Format**

WiSE reads floorplans from text files, which contain a list of walls. Each wall is defined by two 3D coordinates, its axis (usually set to 1 for x-axis), and a wall type.

```
wall index x1 y1 z1 x2 y2 z2 axis type
```

There is a list of pre-defined types, such as sheetrock, concrete, metal, wood, glass, and more. User-defined wall types can be specified by their respective transmission and reflection losses  $\tau$  and  $\rho$ , and their dielectric coefficient  $\epsilon$ , width d and conductivity  $\sigma$ :

```
walltype index {tloss \tau} {rloss \rho} {layers n (\epsilon d \sigma)<sup>n</sup>} {name string}
```

A sample WiSE wall file might look like this:

```
filetype wall
title Sample Floorplan

wall 01 24.9 -34.9 0.0 24.9 -70.1 4.0 1 21

wall 02 24.9 -70.1 0.0 69.8 -70.1 4.0 1 21

wall 03 69.8 -70.1 0.0 69.8 -55.0 4.0 1 21

...

wall 49 42.4 -55.0 0.0 42.4 -58.0 4.0 1 21

wall 50 40.2 -58.0 0.0 40.2 -55.0 4.0 1 21

wall 51 38.0 -55.0 0.0 38.0 -58.0 4.0 1 21

floor 52 6 24.9 -70.1 69.8 -70.1 69.8 -55 44.6 -55 44.6 -34.9 24.9 -34.9 0 21

floor 53 6 24.9 -70.1 69.8 -70.1 69.8 -55 44.6 -55 44.6 -34.9 24.9 -34.9 4 21

walltolerance 0.0001

walltype 21 layers 3 1 0 0 15 1.15 1 1 0 0 name interior_wall
```

# **Bibliography**

- (1) ASCENSION TECHNOLOGY CORPORATION. Flock of Birds: Degrees-of-Freedom Measurement Device.
- (2) BAHL, P., AND PADMANABHAN, V. N. RADAR: An In-Building RF-Based User Location and Tracking System. In *INFOCOM* (2) (2000), pp. 775–784.
- (3) EITER, T., AND MANNILA, H. Computing Discrete Fréchet Distance. Tech. rep., Christian Doppler Laboratory for Expert Systems, Technische Universität Wien, April 1994.
- (4) EKAHAU. Positioning Engine. http://www.ekahau.com/products/positioningengine/.
- (5) ELNAHRAWY, E., LI, X., AND MARTIN, R. P. The Limits of Localization Using Signal Strength: A Comparative Study. In *IEEE SECON* (2004), Rutgers University.
- (6) FORTUNE, S. J., GAY, D. M., KERNIGHAN, B. W., LANDRON, O., VALENZUELA, R. A., AND WRIGHT, M. H. WiSE Design of Indoor Wireless Systems: Practical Computation and Optimization. *IEEE Comput. Sci. Eng. 2*, 1 (1995), 58–68.
- (7) GENTILE, C., AND KLEIN-BERNDT, L. Robust Location using System Dynamics and Motion Constraints. In *IEEE Trans. on Image Processing, Vol. 13, No. 2, pp. 166-178* (Feb. 2004), National Institute of Standards and Technology.
- (8) HÄHNEL, D., BURGARD, W., FOX, D., FISHKIN, K., AND PHILIPOSE, M. Mapping and Localization with RFID Technology. In *Proc. of the IEEE International Conference on Robotics and Automation (ICRA)* (2004).
- (9) HARTER, A., HOPPER, A., STEGGLES, P., WARD, A., AND WEBSTER, P. The Anatomy of a Context-Aware Application. In *Mobile Computing and Networking* (1999), pp. 59–68.
- (10) HASHEMI, H. The Indoor Radio Propagation Channel. In *Proceedings of the IEEE, Vol. 81, No. 7* (July 1993).
- (11) HAYNES, T. A Primer on Digital Beamforming, March 1998.
- (12) HIGHTOWER, J., AND BORRIELLO, G. Location Systems for Ubiquitos Computing. In *IEEE Computer Magazine* (August 2001).

- (13) KASPAR, D. NIST Location System. http://www.antd.nist.gov/wctg/NISTlocation/locationdemo.htm.
- (14) KRUMM, J., CERMAK, G., AND HORVITZ, E. RightSPOT: A Novel Sense of Location for a Smart Personal Object. In *Ubicomp* (2003), pp. 36–43.
- (15) LADD, A., BEKRIS, K., MARCEAU, G., RUDYS, A., WALLACH, D., AND KAVRAKI, L. Using Wireless Ethernet for Localization. ISPIRC-02.
- (16) LADD, A. M., BEKRIS, K. E., RUDYS, A. P., WALLACH, D. S., AND KAVRAKI, L. E. On the Feasibility of Using Wireless Ethernet for Indoor Localization. In *Robotics and Automation, IEEE Transactions* (June 2004).
- (17) ORR, R., AND ABOWD, G. The Smart Floor: A Mechanism for Natural User Identification and Tracking. In *Human Factors in Computing Systems, The Hague, Netherlands* (April 2000).
- (18) Outmesguine, M. Netgear @ CES RangeMax MIMO Wireless Access Point (2005). http://www.engadget.com/entry/1234000803026833.
- (19) PRIYANTHA, N. B., CHAKRABORTY, A., AND BALAKRISHNAN, H. The Cricket Location-Support System. In *Mobile Computing and Networking* (2000), pp. 32–43.
- (20) RUBNER, Y., AND DIXON, S. Earth Mover's Distance Source Code. http://vision.stanford.edu/rubner/.
- (21) RUBNER, Y., TOMASI, C., AND GUIBAS, L. J. The Earth Mover's Distance as a Metric for Image Retrieval. *Int. J. Comput. Vision 40*, 2 (2000), 99–121.
- (22) TSCHICHOLD-GÜRMAN, N., AND CATTIN, P. Recognition of Door-number Plates for Mobile Robot Localisation. *Neuronale Netze in der Anwendung* (1998).
- (23) TSCHICHOLD-GÜRMAN, N., VESTLI, S. J., AND SCHWEITZER, G. Operating Experiences with the Service Robot MoPS, 2001.
- (24) VALENZUELA, R. A., LANDRON, O., AND JACOBS, D. L. Estimating Local Mean Signal Strength of Indoor Multipath Propagation. In *IEEE Transactions on Vehicular Technology, Vol. 46, No. 1* (February 1997).
- (25) WANT, R., HOPPER, A., FALCAO, V., AND GIBBONS, J. The Active Badge Location System. Tech. Rep. 92.1, ORL, 24a Trumpington Street, Cambridge CB2 1QA, 1992.
- (26) WARD, A., JONES, A., AND HOPPER, A. A New Location Technique for the Active Office, 1997.